Published for SISSA by Springer

Received: November 11, 2025
Revised: January 30, 2026
Accepted: March 3, 2026
Published: May 15, 2026

Search for long-lived particles using displaced vertices with low-momentum tracks in proton-proton collisions at $\sqrt{s} = 13$ TeV

The CMS collaboration

Full author list at the end of the paper

E-mail: cms-publication-committee-chair@cern.ch

Abstract: A search for long-lived particles using final states including a displaced vertex with low-momentum tracks, large missing transverse momentum, and a jet from initial-state radiation is presented. This search uses proton-proton collision data at a center-of-mass energy of 13 TeV collected by the CMS experiment at the CERN LHC in 2017 and 2018, with a total integrated luminosity of 100 fb^{-1}. This analysis adopts specific supersymmetric (SUSY) coannihilation scenarios as benchmark signal models, characterized by a next-to-lightest SUSY particle (NLSP) with a mass difference of less than 25 GeV relative to the lightest SUSY particle, assumed to be a bino-like neutralino. In the top squark ($\widetilde{\text{t}}$) NLSP model, the NLSP is a long-lived $\widetilde{\text{t}}$, while in the bino-wino NLSP scenario, the mass-degenerate NLSPs are a wino-like long-lived neutralino and a short-lived chargino. The search excludes top squarks with masses less than 400–1100 GeV and wino-like neutralinos with masses less than 220–550 GeV, depending on the signal parameters, including the mass difference, mass, and lifetime of the long-lived particle. It sets the most stringent limits to date for the $\widetilde{\text{t}}$ and bino-wino NLSP models.

Keywords: Beyond Standard Model, Hadron-Hadron Scattering, Lifetime, Supersymmetry

ArXiv ePrint: 2511.08212

https://doi.org/10.1007/JHEP05(2026)191

Contents

JHEP05(2026)191

1 Introduction

Many theories beyond the standard model (SM) predict long-lived particles (LLPs), whose mean proper lifetimes are longer than ∼0.1 ps, which could be detected by the experiments at the CERN LHC. In some of these models, LLP decays include an invisible particle, which can be a dark-matter candidate, making those models even more appealing. Such models include the top squark ($\widetilde{\mathrm{t}}$) next-to-lightest supersymmetric particle (NLSP) [1, 2] and bino-wino NLSP [3] models. Additionally, a variety of other models predict similar final states, such as split supersymmetry (SUSY) [4–9], stealth SUSY [10, 11], gauge-mediated SUSY breaking [12–14], and hidden valley models [15–17]. Because of their long lifetimes, LLPs can travel a measurable distance in the detector, thus creating unique signatures that enable the possibility to explore new regions of phase space.

This search targets LLPs that propagate between approximately 0.01 and 40 cm before decaying to at least one neutral particle and a number of charged particles. The charged particles from the LLP decays originate from displaced vertices, which can be reconstructed as the common origin point of the trajectories of the charged LLP decay products. In addition, the invisible particles produce missing transverse momentum ($p_{\mathrm{T}}^{\mathrm{miss}}$), while an initial-state radiation (ISR) jet provides the recoil against the LLPs to yield a large $p_{\mathrm{T}}^{\mathrm{miss}}$. As a result, the search signature includes at least one displaced vertex, $p_{\mathrm{T}}^{\mathrm{miss}}$, and a jet from ISR.

The ATLAS and CMS Collaborations have previously performed searches for LLPs using displaced vertices [18–24]. However, event and vertex selections applied in those searches resulted in a reduced sensitivity to scenarios where the mass difference between the LLP and the invisible particle is less than 25 GeV. The search presented in this paper aims to cover this gap, focusing on a mass difference in the range of 12–25 GeV. To enhance the sensitivity to small mass differences, this search makes use of well-measured low-momentum tracks. Because of the improved performance of the upgraded tracker in 2017–2018 and the reduced displaced tracking efficiency resulting from the electronic saturation effect of the

tracker strip readout in 2016 [25], we perform the search using only events collected in 2017 and 2018, corresponding to an integrated luminosity of $100\,\mathrm{fb}^{-1}$.

The $\widetilde{\mathrm{t}}$ [1, 2] and bino-wino [3] NLSP models, illustrated in figure 1, are used as benchmark signal models in this search. In both models, a bino-like neutralino ($\widetilde{\chi}_1^0$) is the lightest SUSY particle (LSP). The NLSP model describes a coannihilation scenario with a $\widetilde{\mathrm{t}}$ ($\overline{\widetilde{\mathrm{t}}}$) as the NLSP. In this model, the $\widetilde{\mathrm{t}}$ is pair produced and long lived, and can decay either via a four-body channel into two fermions (f), a b quark, and a $\widetilde{\chi}_1^0$, or via a two-body channel into a c quark and a $\widetilde{\chi}_1^0$. According to the theoretical predictions, the $\widetilde{\mathrm{t}}$ mass ($m_{\widetilde{\mathrm{t}}}$), the mass difference between the NLSP and LSP (Δm), and the branching fraction of the four-body decay $\mathcal{B}(\widetilde{\mathrm{t}} \to \mathrm{bf}\overline{\mathrm{f}}'\widetilde{\chi}_1^0)$ can be treated as free parameters, while the $\widetilde{\mathrm{t}}$ proper decay length ($c\tau$) depends on the other parameters. The decay width of the four-body decay $\Gamma(\widetilde{\mathrm{t}} \to \mathrm{bf}\overline{\mathrm{f}}'\widetilde{\chi}_1^0)$ is given by ref. [1] as:

$$\Gamma(\widetilde{\mathrm{t}} \to \mathrm{bf}\overline{\mathrm{f}}'\widetilde{\chi}_1^0) = 252\,\mathrm{cm}^{-1} \left(\frac{\Delta m}{30\,\mathrm{GeV}}\right)^8 \left(\frac{400\,\mathrm{GeV}}{m_{\widetilde{\mathrm{t}}}}\right), \tag{1.1}$$

with $c\tau = \mathcal{B}(\widetilde{\mathrm{t}} \to \mathrm{bf}\overline{\mathrm{f}}'\widetilde{\chi}_1^0)/\Gamma(\widetilde{\mathrm{t}} \to \mathrm{bf}\overline{\mathrm{f}}'\widetilde{\chi}_1^0)$. For different fermion flavors in the four-body decay, the corresponding decay widths follow the relationships from ref. [1], where ℓ represents a charged lepton (e, μ, or τ):

$$\Gamma(\widetilde{\mathrm{t}} \to \mathrm{bu}\overline{\mathrm{d}}\widetilde{\chi}_1^0) \approx \Gamma(\widetilde{\mathrm{t}} \to \mathrm{bc}\overline{\mathrm{s}}\widetilde{\chi}_1^0) \approx 3\Gamma(\widetilde{\mathrm{t}} \to \mathrm{b}\ell^+\nu_\ell\widetilde{\chi}_1^0). \tag{1.2}$$

When Δm is less than approximately 25 GeV, $c\tau$ becomes sufficiently long to lead to the production of displaced vertices. By requiring one or more displaced vertices, the analysis is sensitive to the scenarios in which the top squarks are long-lived.

The bino-wino NLSP model predicts a nearly mass-degenerate wino-like chargino $\widetilde{\chi}_1^\pm$ and a neutralino $\widetilde{\chi}_2^0$ as the NLSPs. In this scenario, the $\widetilde{\chi}_1^\pm$ decays promptly to a $\mathrm{W}^\pm$ boson and a $\widetilde{\chi}_1^0$, since the decay happens via a dimension-five operator. When the Δm between the NLSP and LSP is less than the Z boson mass, the $\widetilde{\chi}_2^0$ predominantly decays through an off-shell Z or H boson, producing a pair of fermions and a $\widetilde{\chi}_1^0$. Both decay channels are suppressed because of the large higgsino mass parameter, rendering the $\widetilde{\chi}_2^0$ long-lived. In this search, only $\widetilde{\chi}_2^0$ decays mediated by the Z boson are considered. Pair production of $\widetilde{\chi}_2^0$ is not considered, since in the pure wino scenario, neutralinos do not couple to the SM Z boson at tree level [26]. This suppresses the neutral current production mechanism for $\widetilde{\chi}_2^0$ pairs. For the statistical interpretation, the masses of $\widetilde{\chi}_1^\pm$ and $\widetilde{\chi}_2^0$, the Δm between the NLSP and LSP, and the $c\tau$ of the $\widetilde{\chi}_2^0$ are all treated as free parameters. Previous searches by the ATLAS and CMS Collaborations [27, 28] have explored this model. However, by exploiting displaced signatures, the present search can probe previously inaccessible regions of the parameter space.

The paper is organized as follows. Section 2 provides an overview of the CMS detector. Section 3 describes the data, simulation, and event selections used in this search. The vertex reconstruction and selection are discussed in section 4. Section 5 presents the definitions of the signal regions (SRs) and the background estimation procedure. Section 6 reviews the systematic uncertainties associated with the signal efficiency and the background estimate. The results and statistical interpretation are discussed in section 7. Finally, section 8 summarizes the paper. Tabulated results are provided in the HEPData record for this analysis [29].

JHEP05(2026)191

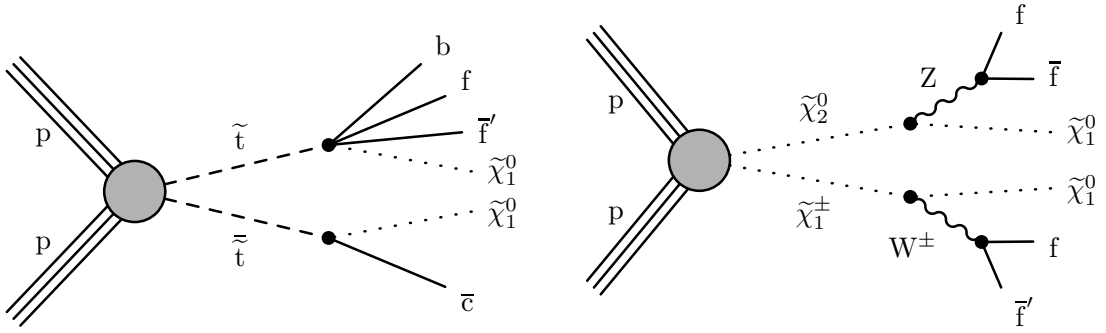

Figure 1. Feynman diagrams for the $\widetilde{t}$ NLSP (left) and the bino-wino NLSP (right) production.

2 The CMS detector

The CMS apparatus [30, 31] is a multipurpose, nearly hermetic detector, designed to trigger on [32–34] and identify electrons, muons, photons, and (charged and neutral) hadrons [35–37]. Its central feature is a superconducting solenoid of 6 m internal diameter, providing a magnetic field of 3.8 T. Within the solenoid volume are a silicon pixel and strip tracker, a lead tungstate crystal electromagnetic calorimeter (ECAL), and a brass and scintillator hadron calorimeter (HCAL), each composed of a barrel and two endcap sections. Forward calorimeters extend the pseudorapidity (η) coverage provided by the barrel and endcap detectors. Muons are reconstructed using gas-ionization detectors embedded in the steel flux-return yoke outside the solenoid. More detailed descriptions of the CMS detector, together with a definition of the coordinate system used and the relevant kinematic variables, can be found in refs. [30, 31].

At the start of 2017, a new pixel detector was installed [38]; the upgraded tracker measured charged particles within the range $|\eta| < 3.0$, covering the radius between 4 and 110 cm. During the LHC running period when the data used in this paper were recorded, the silicon tracker consisted of 1856 silicon pixel and 15 148 silicon strip detector modules. For nonisolated particles with transverse momentum (p_T) in the range $1 < p_T < 10$ GeV and $|\eta| < 3.0$, the track resolutions are typically 1.5% in p_T and 20–75 μm in the transverse impact parameter (d_{xy}) [37, 39].

Events of interest are selected using a two-tiered trigger system. The first level, referred to as the level-1 (L1) trigger, is composed of custom hardware processors and uses information from the calorimeters and muon detectors to select events at a rate of around 100 kHz within a fixed latency of about 4 μs [33]. The second level, known as the high-level trigger, consists of a farm of processors running a version of the full event reconstruction software optimized for fast processing and reduces the event rate to around 1 kHz before data storage [32, 33].

A particle-flow (PF) algorithm [40] aims to reconstruct and identify each individual particle in an event, with an optimized combination of information from the various elements of the CMS detector. The energy of photons is obtained from the ECAL measurement. The energy of electrons is determined from a combination of the electron momentum at the primary interaction vertex, as determined in the tracker, the energy of the corresponding ECAL cluster, and the energy sum of all bremsstrahlung photons spatially compatible with originating from the electron track. The energy of muons is obtained from the curvature of

JHEP05(2026)191

the corresponding track. The energy of charged hadrons is determined from a combination of their momentum measured in the tracker and the matching ECAL and HCAL energy deposits, corrected for the response function of the calorimeters to hadronic showers. Finally, the energy of neutral hadrons is obtained from the corresponding corrected ECAL and HCAL energies. The primary vertex is taken to be the vertex corresponding to the hardest scattering in the event, evaluated using tracking information alone, as described in section 9.4.1 of ref. [41].

For each event, hadronic jets are clustered from PF candidates using the infrared- and collinear-safe anti-k_{T} algorithm [42, 43] with a distance parameter of 0.4. Jet momentum is determined as the vectorial sum of all particle momenta in the jet, and is found from simulation to be, on average, within 5–10% of the true momentum over the entire p_{T} spectrum and detector acceptance. Additional proton-proton interactions within the same or nearby bunch crossings (referred to as pileup) can contribute additional tracks and calorimetric energy depositions to the jet momentum. To mitigate this effect, charged particles identified as originating from pileup vertices are discarded, and an offset correction is applied to correct for remaining contributions [44]. Jet energy corrections are derived from simulation to bring the measured response of jets to that of particle-level jets on average. In situ measurements of the momentum balance in dijet, photon+jet, Z+jet, and multijet events are used to account for any residual differences in the jet energy scale between data and simulation [45]. The jet energy resolution amounts typically to 15–20% at 30 GeV, 10% at 100 GeV, and 5% at 1 TeV [45]. Additional selection criteria are applied to remove jets potentially dominated by anomalous contributions from various subdetector components or reconstruction failures [46]. To identify jets originating from b quark fragmentation (b jets), the "tight" working point of the DeepJet tagging algorithm is used, which has an identification efficiency for b jets from top quark decays with $p_{\mathrm{T}} > 30$ GeV of about 58% and a misidentification probability for light jets (from the fragmentation of u, d, s quarks and gluons) of about 0.1% [47–49].

The $\vec{p}_{\mathrm{T}}^{\,\mathrm{miss}}$ is computed as the negative vector p_{T} sum of all the PF candidates in an event, and its magnitude is denoted as $p_{\mathrm{T}}^{\mathrm{miss}}$ [50]. The $\vec{p}_{\mathrm{T}}^{\,\mathrm{miss}}$ is modified to account for corrections to the energy scale of the reconstructed jets in the event. Anomalous events with high $p_{\mathrm{T}}^{\mathrm{miss}}$ can be due to a variety of reconstruction failures, detector malfunctions, or noncollision backgrounds. Such events are rejected by event filters that are designed to identify more than 85–90% of the spurious high-$p_{\mathrm{T}}^{\mathrm{miss}}$ events with a mistagging rate less than 0.1% [50].

Hadronic τ lepton decays (τ_{h}) are reconstructed from jets using the hadrons-plus-strips algorithm [51], which combines one or three tracks with energy deposits in the calorimeters to identify the τ decay modes.

3 Preselection and event samples

Events used in this search are required to pass a preselection, designed to select events with a high-p_{T} ISR jet and large $p_{\mathrm{T}}^{\mathrm{miss}}$. These events are recorded by a trigger requiring $p_{\mathrm{T}}^{\mathrm{miss}} > 120$ GeV and are required to have offline $p_{\mathrm{T}}^{\mathrm{miss}} > 400$ GeV, which removes background events, while retaining signal events. In addition, events are required to have at least one jet with $p_{\mathrm{T}} > 100$ GeV and $|\eta| < 2.4$. The highest p_{T} jet in an event is considered the ISR candidate jet. The preselection also rejects events containing well-reconstructed muon, electron, photon, or hadronically decaying τ candidates that satisfy the following requirements.

JHEP05(2026)191

Muons must have $p_T > 10\,\text{GeV}$ and $|\eta| < 2.4$ [36]. Electrons are required to have $p_T > 10\,\text{GeV}$ and $|\eta| < 2.5$ [35]. Photons must have $p_T > 15\,\text{GeV}$ and $|\eta| < 2.5$ [35]. Tau leptons are required to have $p_T > 18\,\text{GeV}$ and $|\eta| < 2.3$ [51]. No requirements are imposed on the degree of detector activity in the vicinity of any such lepton or photon. This veto allows for the amount of background to be reduced by a factor of two.

Signal events are simulated at leading order (LO) using MadGraph5_aMC@NLO 2.6.5 [52], with up to two additional jets included in the matrix element calculations. The MLM [53] prescription is used to match jets from matrix element calculations to those from parton showers. The LLP production cross sections are normalized to next-to-next-to-LO (NNLO) accuracy in quantum chromodynamics (QCD) and matched to next-to-next-to-leading logarithmic (NNLL) soft-gluon resummation [54]. For the $\widetilde{\mathrm{t}}$ NLSP model, bound states resulting from the color charges carried by $\widetilde{\mathrm{t}}$ could have kinematic effects and interact with materials in the detector. The interactions follow the cloud model [55, 56] in the simulation. The $\widetilde{\mathrm{t}}$ NLSP samples are generated with different $\widetilde{\mathrm{t}}$ masses ranging from 400 to 1400 GeV, with Δm ranging from 12 to 25 GeV, and $\mathcal{B}(\widetilde{\mathrm{t}} \to \mathrm{bf}\bar{\mathrm{f}}'\widetilde{\chi}_1^0)$ ranging from 10 to 100%, corresponding to $c\tau$ in the range of 0.01–400 mm. The lower bound on Δm is set to 12 GeV, as smaller values of Δm correspond to $c\tau$ ranges where the search sensitivity diminishes. The bino-wino NLSP samples are generated with different masses of the NLSP ranging from 200 to 600 GeV, with Δm ranging from 12 to 25 GeV, and $c\tau$ ranging from 0.2 to 200 mm.

As a result of the significant p_T^{miss} requirement, the dominating background processes include Z and W boson production in association with up to four jets from the matrix element calculations (Z/W+jets), where the Z boson decays to neutrino-antineutrino pairs and the W boson decays to a lepton and its corresponding neutrino. Additional contributions arise from $\mathrm{t\bar{t}}$, events with jets produced through the strong interaction (QCD events), and single top quark production. The Z/W+jets and QCD events are generated using MadGraph5_aMC@NLO at LO, with the MLM [53] prescription for jet matching applied. The $\mathrm{t\bar{t}}$ events are generated using MadGraph5_aMC@NLO 2.6.1 at next-to-LO (NLO), with the FxFx [57] prescription for jet matching. Single top quark production is generated using powheg [58–62] (version 2.0 for t-channel and 1.0 for tW-channel production) at NLO in QCD, and the diboson processes are generated with pythia 8.240 [63]. Simulated background events are used solely for selection optimization and systematic uncertainty studies and are not employed in the search results, as the background is evaluated from data.

The NNPDF3.1 NNLO [64, 65] set of parton distribution functions (PDFs) is used for all simulated samples. The MadGraph5_aMC@NLO and powheg generators are interfaced with pythia with the underlying event tune CP5 [66] to model parton showering and fragmentation.

For all the simulated events, Geant4 [67] is used to simulate the CMS detector response. To describe the effect of pileup, simulated minimum bias events are superimposed on the hard interactions, with the multiplicity matching that observed in data.

4 Displaced vertex reconstruction

Displaced vertices are found using well-reconstructed and displaced tracks. A track is considered well reconstructed if it has $p_T > 0.5\,\text{GeV}$, at least six associated tracker hits, a normalized $\chi^2 < 5$, which represents the compatibility between the measured tracker hit

JHEP05(2026)191

positions and the positions predicted by the fitted track, and a relative uncertainty in p_{T} less than 1.5%. The displacement criterion requires a track to satisfy S_{xy}^{trk} to be at least 2, where S_{xy}^{trk} is defined as the ratio of the d_{xy} to its associated uncertainty and is calculated with respect to the primary vertex.

Displaced vertices are reconstructed by the inclusive vertex finder (IVF) [47], which is based on the adaptive vertex fitter [68]. In the IVF method, the selected tracks are sorted into multiple clusters based on the distance of the closest approach between tracks. The adaptive vertex fitter is then applied iteratively to each cluster to find the candidates for displaced vertices. During the fitting process, multiple displaced vertices can be fit in a single cluster, and tracks are assigned to vertices with weights reflecting the likelihood that each track originates from a given vertex. A deterministic annealing algorithm is applied to obtain a robust fit result. Vertex candidates are further merged if they share more than 70% of their associated tracks and if their separation satisfies $d_{\mathrm{vv}}/\sigma_{d_{\mathrm{vv}}} < 2$, where d_{vv} is the distance between the vertices and $\sigma_{d_{\mathrm{vv}}}$ is its associated uncertainty. To obtain optimally reconstructed vertices, an arbitration step is performed to assign tracks to vertex candidates when they are in close proximity. In this step, the distance between unassociated tracks and reconstructed vertices is evaluated. Tracks found to be sufficiently close to a vertex are added to it, followed by a vertex refit. This procedure effectively "recycles" tracks that were not already included in vertices, thereby enhancing the overall vertex reconstruction performance. Following the track arbitration, an additional merging step is performed to prevent track sharing: vertex candidates are merged if their distance divided by their uncertainty is less than 10 and they share more than 20% of their tracks. Each time the set of tracks in a vertex is updated, the vertex is refitted.

For this search, parameters of the IVF are tuned to allow vertices with tracks that have large angular separation, thus enhancing the reconstruction efficiency for LLP decays with large opening angles between the decay products and large $p_{\mathrm{T}}^{\mathrm{miss}}$. The reconstruction efficiency, defined as the fraction of LLPs that are reconstructed as displaced vertices, is shown in figure 2 as a function of LLP transverse displacement. The results are presented for bino-wino NLSP samples with an LLP mass (m_{LLP}) of 400 GeV, $c\tau = 20$ mm, and $\Delta m = 25$ and 12 GeV. The tuned IVF shows significantly improved efficiency compared with the default configuration across both Δm values and displacement ranges. The reconstruction efficiency rises with increasing transverse displacement up to a few centimeters, then gradually decreases because of reduced tracking and vertexing performance at larger displacements.

Figure 3 shows the key features of a displaced vertex. The transverse distance between the primary and displaced vertices is referred to as L_{xy}. The displacement vector is defined as the vector pointing from the primary to the displaced vertex. The vertex momentum is calculated as the vector sum of the momenta of all tracks at the vertex. The three-dimensional angle between the displacement vector and the vertex momentum is referred to as α_{p}.

The reconstructed displaced vertices can include background vertices resulting from the SM LLPs, such as b hadrons, nuclear interactions between particles and materials in the detector, and random crossings of unrelated tracks. Background vertices are removed by applying selection criteria to both the tracks associated with the vertices and the vertices themselves.

JHEP05(2026)191

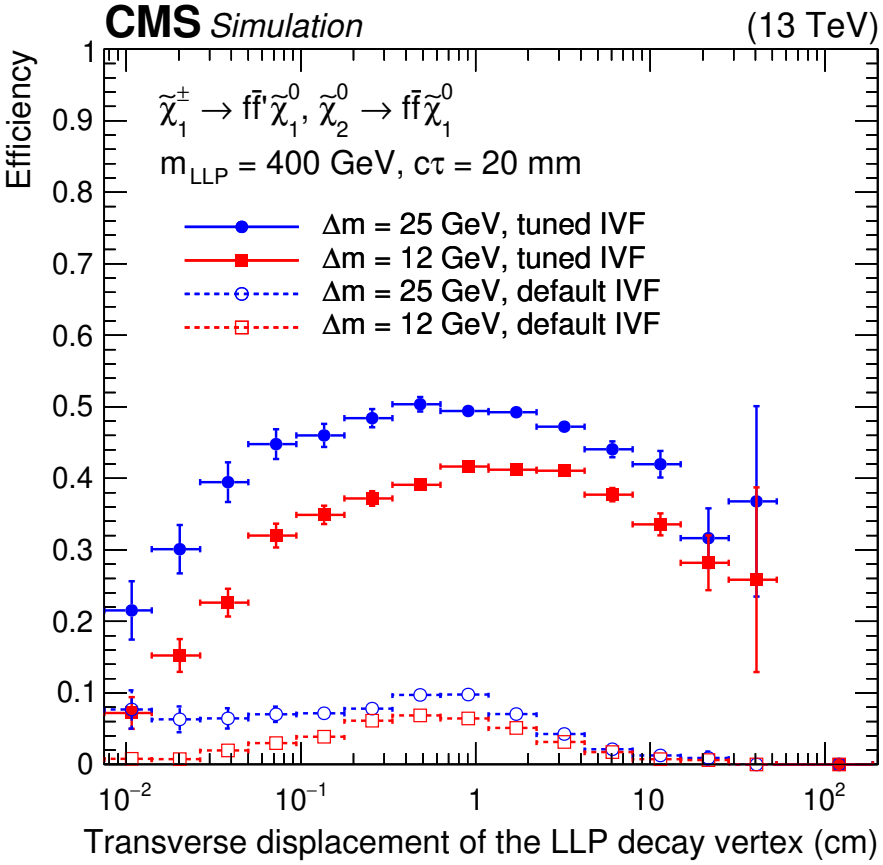

Figure 2. The LLP reconstruction efficiency as a function of the transverse displacement of the LLP decay vertex. Bino-wino NLSP samples with $m_{\mathrm{LLP}} = 400\,\mathrm{GeV}$, $c\tau = 20\,\mathrm{mm}$, and $\Delta m = 25$ (blue circles) and 12 (red squares) GeV are shown in the plot. Tuned (solid) and default (dashed) IVF are compared.

A "good track" must satisfy the following criteria. The number of associated detector hits measured in the tracker must be greater than 13, which ensures that the track is well measured. To remove tracks from pileup vertices, the absolute value of the ratio between d_{xy} and the longitudinal impact parameter (d_z) must be greater than 0.25. Given the recoil of the ISR jet, LLP decay products tend to be in the same hemisphere as the $\vec{p}_{\mathrm{T}}^{\,\mathrm{miss}}$ and the opposite hemisphere of the ISR jet. As a result, the difference in the azimuthal angle (ϕ) between the track and $\vec{p}_{\mathrm{T}}^{\,\mathrm{miss}}$ ($\Delta\phi(\mathrm{trk}, \vec{p}_{\mathrm{T}}^{\,\mathrm{miss}})$) is required to be less than 1.5 radians, while the ϕ difference between the track and the ISR jet candidate ($\Delta\phi(\mathrm{trk}, \mathrm{ISR})$) is required to be greater than 1. To reject tracks within jets, we calculate the track isolation, defined as the scalar sum of the transverse energy of charged hadrons, neutral hadrons, and photons within a cone of $\Delta R = 0.3$, where $\Delta R \equiv \sqrt{(\Delta\phi)^2 + (\Delta\eta)^2}$ corresponds to the angular distance between the track and each particle considered in the sum. The ratio of the track isolation to the track p_{T} is required to be less than 5. In addition, we require tracks to have S_{xy}^{trk} greater than 4 to further remove prompt background tracks.

The following selections on vertex features are also applied. The number of degrees of freedom, calculated as two times the sum of track weights, less 3, must be greater than

JHEP05(2026)191

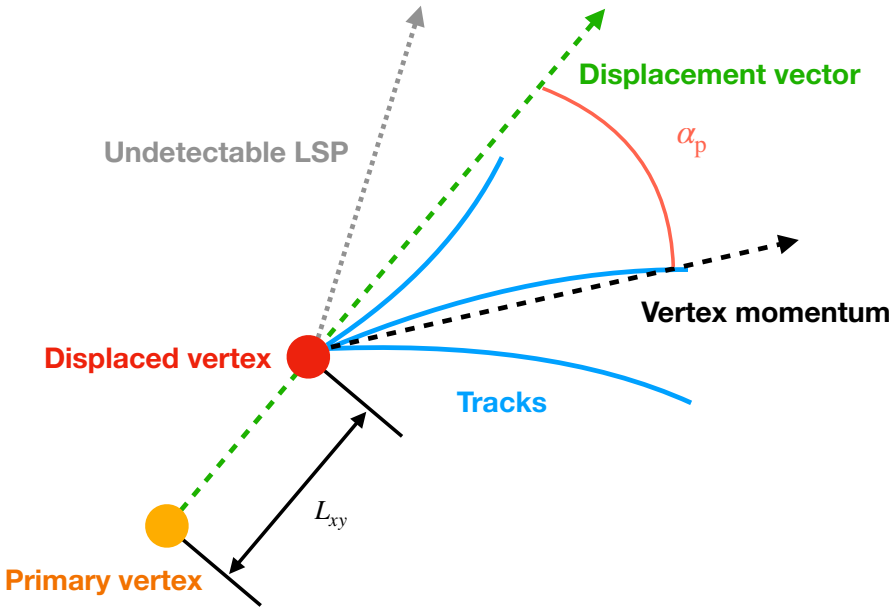

Figure 3. Diagram that shows the key features of a displaced vertex.

1, which ensures the vertices are well reconstructed. Following the same argument as the good track selection, the ϕ difference between the vertex displacement vector and $\vec{p}_{\mathrm{T}}^{\,\mathrm{miss}}$ ($\Delta\phi(\mathrm{vtx}, \vec{p}_{\mathrm{T}}^{\,\mathrm{miss}})$) is required to be less than 1.5, and the ϕ difference between the vertex displacement vector and the ISR jet candidate ($\Delta\phi(\mathrm{vtx}, \mathrm{ISR})$) is required to be greater than 1. In addition, the number of tracks that satisfy $|d_{xy}/d_z|$ greater than 0.25 must be at least one to remove vertices from pileup. To make the search sensitive to LLPs with different lifetimes, no explicit selection on vertex L_{xy} is applied. Figure 4 compares the α_{p} distribution for vertices that satisfy the aforementioned selections in data, simulated background, and signal from the bino-wino NLSP sample with $m_{\mathrm{LLP}} = 400\,\mathrm{GeV}$, $c\tau = 20\,\mathrm{mm}$, and $\Delta m = 15\,\mathrm{GeV}$. It shows that a large fraction of background vertices have a value of α_{p} close to 0. A selection of $\alpha_{\mathrm{p}} > 0.2$ is imposed. This threshold is optimized to maximize the search sensitivity based on the event yields in the SRs and is not directly derived from figure 4. To reduce model dependence, no upper bound is imposed on α_{p}. Comparing data and background simulation, we find that data vertices tend to have larger α_{p}. This discrepancy arises from the mismodeling of pileup, as vertices in data are more likely to include additional tracks originating from pileup interactions, which in turn lead to higher α_{p} values.

To remove vertices that result from nuclear interactions of SM particles with the tracker material, we veto vertices whose positions are consistent with originating within the tracker material. To this end, we derived a material map from the positions of displaced vertex candidates in 2017 and 2018 data. Events that satisfy the $p_{\mathrm{T}}^{\mathrm{miss}}$ trigger with a minimum threshold of 120 GeV and pass the noise filters [50] are used for this purpose. To avoid potential bias, events that contribute to the SRs defined in section 5 are excluded in the derivation of the map. In each event, displaced vertices are reconstructed and required to have at least two tracks and greater than one degree of freedom. The map is obtained by projecting all of the selected vertices onto the plane transverse to the beam. To remove vertices from SM

JHEP05(2026)191

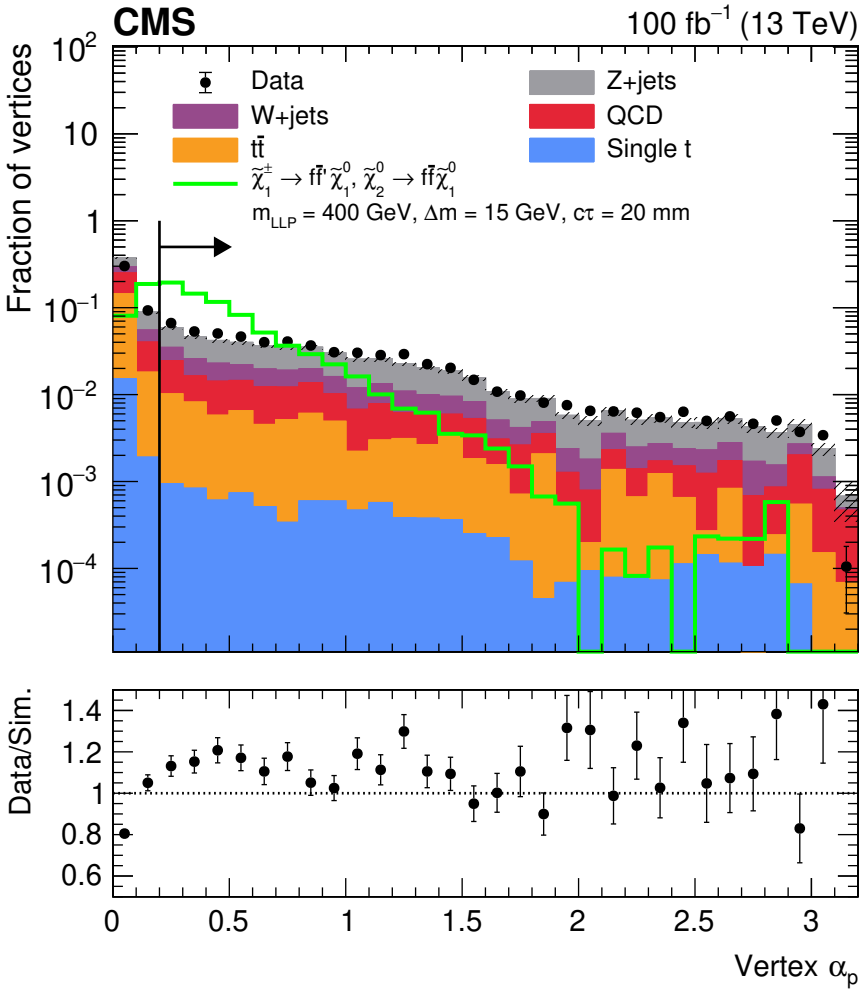

Figure 4. The vertex α_p distribution compared between data, simulation, and bino-wino NLSP sample with $m_{LLP} = 400\,\text{GeV}$, $c\tau = 20\,\text{mm}$, and $\Delta m = 15\,\text{GeV}$. All distributions are normalized to unity. The ratio of data to simulation is shown in the lower panel. The arrow indicates the value of the optimal α_p threshold.

LLP decays and random track crossings, a requirement on the vertex density as a function of the transverse radius is applied to exclude regions with fewer vertices. The resulting map is shown in figure 5. A similar study was performed in ref. [21], and the resulting maps are found to be consistent. The map is applied to both data and simulated events. The material map veto reduces the signal efficiency by 0–10%, depending on the lifetime of the LLP.

Vertices that meet the criteria based on the vertex features and are not vetoed by the material map are said to have passed the vertex selections and are used in the analysis.

5 Event selection and background estimation

In addition to the preselection defined in section 3, events with at least one vertex that satisfies the vertex selections are further divided into four exclusive categories based on the number of good tracks. Events containing at least one vertex with at least three good

JHEP05(2026)191

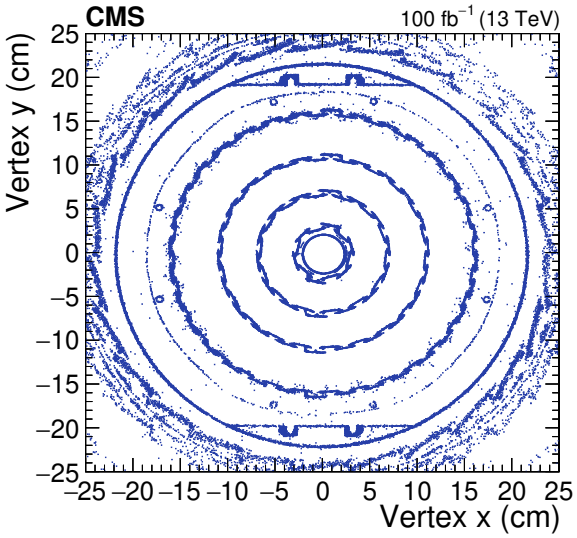

Figure 5. Material map for the CMS tracker derived from data. A zoomed-in view is provided for x and y within the range -25 to 25 cm.

tracks are assigned to the tight signal plane. Those with at least one vertex containing exactly two good tracks, and not satisfying the tight signal plane criteria, are assigned to the medium signal plane. The remaining events with at least one vertex with one good track are assigned to the loose signal plane. Events with vertices with no good tracks are classified into the control plane. Within each plane, four regions are defined based on whether the requirements $p_{\mathrm{T}}^{\mathrm{miss}} > 700\,\mathrm{GeV}$ and $S_{xy}^{\mathrm{vtx}} > 20$, where S_{xy}^{vtx} denotes the ratio of the vertex transverse displacement L_{xy} to its uncertainty, are satisfied. The S_{xy}^{vtx} and $p_{\mathrm{T}}^{\mathrm{miss}}$ variables are found to be statistically independent for the background processes. The selections are optimized to achieve the maximum sensitivity to the benchmark signal models. In events with more than one vertex, the vertex with the greatest S_{xy}^{vtx} is used. The definition of the regions is illustrated in figure 6. The SRs include all regions in the tight and medium signal plane, and regions A and C in the loose signal plane. All other regions are used as control regions (CRs), including regions B and D in the loose signal plane and all regions in the control plane.

This search adopts a novel background estimation method using transfer factors, which is purely based on data. The overall strategy consists of multiplying the number of events in the control plane by transfer factors to predict the number of events in other planes. Because of the $S_{xy}^{\mathrm{trk}} > 4$ requirement in the good track selection, S_{xy}^{vtx} and the number of good tracks are statistically dependent. To mitigate the impact of this dependence, the background estimation is performed without the S_{xy}^{vtx} selection. Instead, predictions are made for a given $p_{\mathrm{T}}^{\mathrm{miss}}$ range and the number of good tracks to ensure a more reliable estimation.

To predict the number of events without S_{xy}^{vtx} selection, a transfer factor ($f_{i\to j}$) is defined as the ratio of events in the target plane with j good tracks to those in the original plane with i good tracks. These transfer factors are computed using events in the low-$p_{\mathrm{T}}^{\mathrm{miss}}$ region ($200 < p_{\mathrm{T}}^{\mathrm{miss}} < 400\,\mathrm{GeV}$), as shown by eq. (5.1). The transfer factor for transitioning from zero to one good track is derived from CRs B0, D0, B1, and D1 in the nominal search planes, as shown by eq. (5.2). Additionally, the transfer factors obtained from low-$p_{\mathrm{T}}^{\mathrm{miss}}$

JHEP05(2026)191

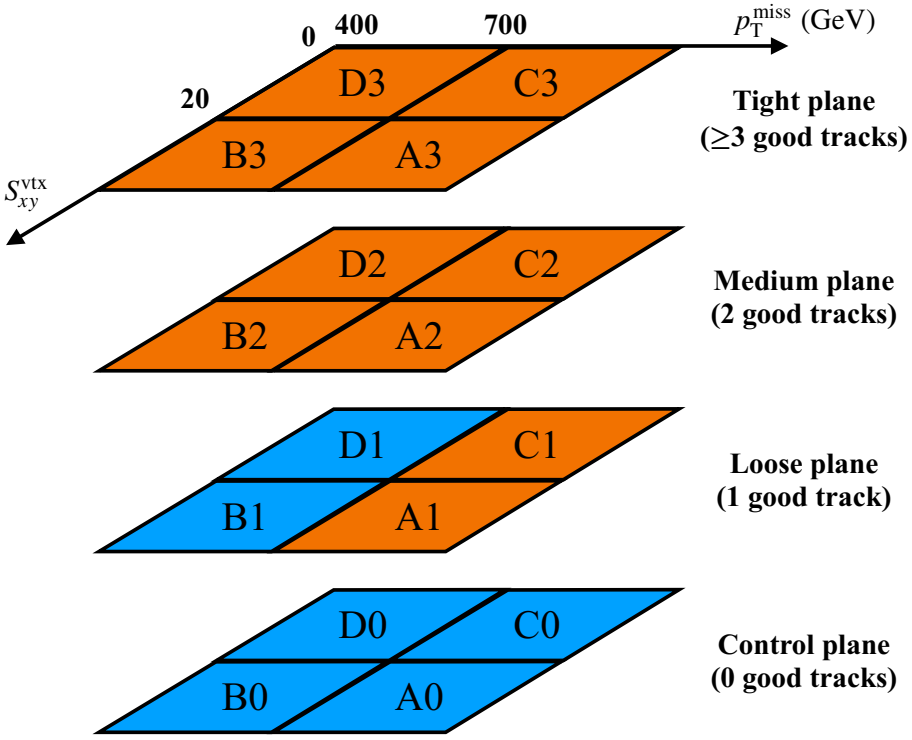

Figure 6. Definition of the signal (orange) and control (blue) regions. Different planes are defined based on the number of good tracks in the vertex. In each plane, different regions are divided according to the $p_{\mathrm{T}}^{\mathrm{miss}}$ and S_{xy}^{vtx} values. The letters in the boxes correspond to the region labels described in the text, while the numbers in the boxes correspond to the plane numbers.

events are scaled by the ratio of transfer factors between the search planes (zero to one good track) and the low-$p_{\mathrm{T}}^{\mathrm{miss}}$ planes, as shown by eq. (5.3). The estimated event yield is then obtained by multiplying the number of events in the CRs by the corresponding transfer factors, as shown by eqs. (5.4) and (5.5).

$$f_{i\to j}^{\text{low-}p_{\mathrm{T}}^{\mathrm{miss}}} = \frac{N_{\mathrm{bkg}}^{j\,\text{good track}}}{N_{\mathrm{bkg}}^{i\,\text{good track}}} \qquad (i,j) = (0,1),(1,2),(2,3). \tag{5.1}$$

$$f_{0\to 1} = \frac{N_{\mathrm{bkg}}^{\mathrm{B1+D1}}}{N_{\mathrm{bkg}}^{\mathrm{B0+D0}}}. \tag{5.2}$$

$$f_{i\to i+1} = \frac{f_{0\to 1}}{f_{0\to 1}^{\text{low-}p_{\mathrm{T}}^{\mathrm{miss}}}} f_{i\to i+1}^{\text{low-}p_{\mathrm{T}}^{\mathrm{miss}}} \qquad i = 1,2. \tag{5.3}$$

$$N_{\mathrm{bkg}}^{\mathrm{A}i\mathrm{+C}i} = N_{\mathrm{bkg}}^{\mathrm{A0+C0}} \prod_{j=0}^{i-1} f_{j\to j+1} \qquad i = 1,2,3. \tag{5.4}$$

$$N_{\mathrm{bkg}}^{\mathrm{B}i\mathrm{+D}i} = N_{\mathrm{bkg}}^{\mathrm{B1+D1}} \prod_{j=1}^{i-1} f_{j\to j+1} \qquad i = 2,3. \tag{5.5}$$

After obtaining event counts for a given $p_{\mathrm{T}}^{\mathrm{miss}}$ range and number of good tracks, the prediction for events with the S_{xy}^{vtx} selection is made. The S_{xy}^{vtx} distributions for each plane are extracted

JHEP05(2026)191

from low-$p_{\mathrm{T}}^{\mathrm{miss}}$ events ($200 < p_{\mathrm{T}}^{\mathrm{miss}} < 400\,\mathrm{GeV}$) in data and used as proxies for the nominal search planes. Studies indicate that the S_{xy}^{vtx} distribution for a given plane remains consistent across different $p_{\mathrm{T}}^{\mathrm{miss}}$ ranges, justifying the use of low-$p_{\mathrm{T}}^{\mathrm{miss}}$ events as a representative sample. From these distributions, for a given plane with i good tracks, the fractions of events satisfying the S_{xy}^{vtx} selection (f_i^{vtx}) are computed. The final background prediction is obtained by multiplying this fraction by the previously estimated total number of events, yielding predictions across all SRs. The calculations are shown by eqs. (5.6)–(5.9).

$$N_{\mathrm{bkg}}^{\mathrm{A}i} = N_{\mathrm{bkg}}^{\mathrm{A}i+\mathrm{C}i} f_i^{\mathrm{vtx}} \qquad i = 1, 2, 3. \tag{5.6}$$

$$N_{\mathrm{bkg}}^{\mathrm{C}i} = N_{\mathrm{bkg}}^{\mathrm{A}i+\mathrm{C}i} \left(1 - f_i^{\mathrm{vtx}}\right) \qquad i = 1, 2, 3. \tag{5.7}$$

$$N_{\mathrm{bkg}}^{\mathrm{B}i} = N_{\mathrm{bkg}}^{\mathrm{B}i+\mathrm{D}i} f_i^{\mathrm{vtx}} \qquad i = 2, 3. \tag{5.8}$$

$$N_{\mathrm{bkg}}^{\mathrm{D}i} = N_{\mathrm{bkg}}^{\mathrm{B}i+\mathrm{D}i} \left(1 - f_i^{\mathrm{vtx}}\right) \qquad i = 2, 3. \tag{5.9}$$

To validate the background estimation method, orthogonal validation planes are constructed by applying different requirements of $\Delta\phi(\mathrm{trk/vtx}, \vec{p}_{\mathrm{T}}^{\mathrm{miss}}/\mathrm{ISR})$. Specifically, it is required that $\Delta\phi(\mathrm{trk/vtx}, \vec{p}_{\mathrm{T}}^{\mathrm{miss}}) > 1.5$ and $\Delta\phi(\mathrm{trk/vtx}, \mathrm{ISR}) > 0.4$. These selections ensure that there is no overlap with the SR and that the vertex is not within the ISR jet area. Figure 7 compares the observation and prediction for regions in the validation planes. It presents the predicted central values along with their associated uncertainties. In the CRs, no predictions are made. For most of the regions in the validation planes, the prediction and observation agree within statistical uncertainties.

6 Systematic uncertainties

The impact of systematic uncertainties associated with the background estimation and the signal efficiency, expressed as the resulting changes in the event yields, is summarized in table 1.

As described in section 5, the background is estimated from data. Therefore, the modeling of the background in simulation has no impact on the analysis. For $f_{0\to1}$ and f_i^{vtx}, the statistical uncertainty in the derivation is used as a systematic uncertainty of up to 2%. The prediction and observation when performing the background estimate procedure in the validation plane defined in section 5 are consistent within the statistical uncertainties, so we apply no additional systematic uncertainty associated with the background estimation.

Systematic uncertainties associated with the signal efficiency result from the modeling of displaced tracks and vertex reconstruction, the accuracy of the material map, jet energy scale, jet energy resolution, unclustered energy, pileup, trigger, lepton and photon veto, integrated luminosity, and the running conditions.

The displaced track and vertex reconstruction efficiency is studied by reconstructing displaced vertices from $\mathrm{K}_{\mathrm{S}}^0 \to \pi^-\pi^+$ decays [69]. Events that satisfy the event preselection described in section 3 are used in the study. Vertices are reconstructed using the algorithms described in section 4. To select $\mathrm{K}_{\mathrm{S}}^0$ decay candidates, vertices are required to have exactly two tracks with opposite charges. In addition, the vertex α_{p} is required to be less than 0.2, so the vertices used in this study do not overlap with the SRs. The distributions of

JHEP05(2026)191

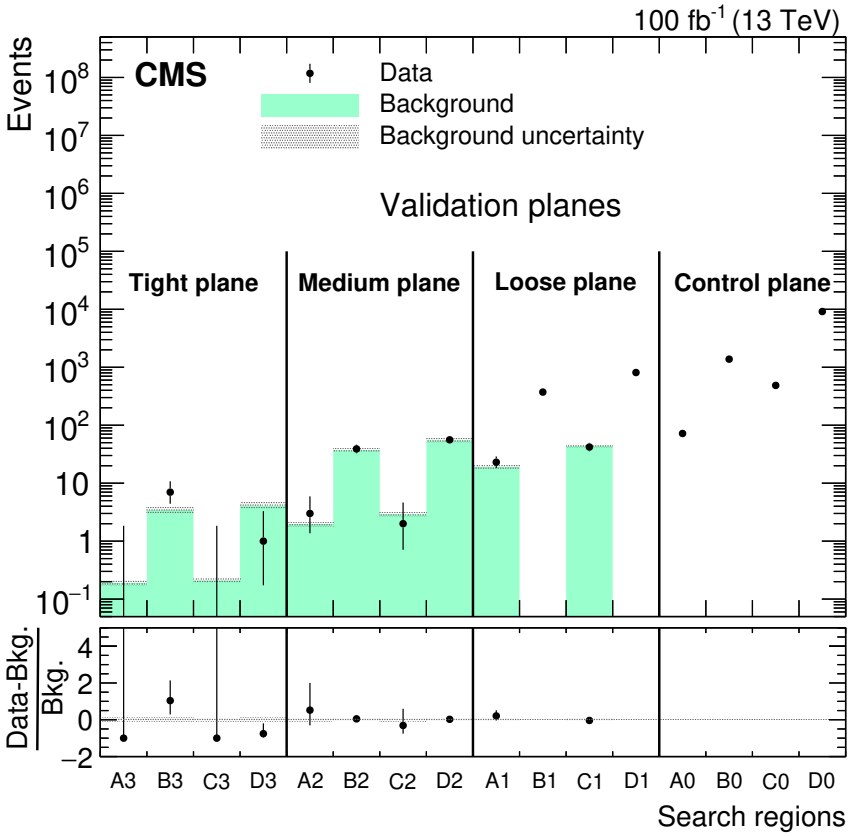

Figure 7. The number of observed and predicted background events in the regions of the validation planes. The predicted background is shown with its associated uncertainties. The observed data are displayed with the 68% Poisson intervals. The lower panel shows the fractional difference between the observed data and the predicted background.

vertex L_{xy} are compared between data and simulation. The L_{xy} distribution is obtained by a fit-based background subtraction performed in each L_{xy} bin. For each bin of L_{xy}, the invariant mass of a vertex, defined as the invariant mass of the two tracks assuming the charged pion mass hypothesis, is required to be between 0.440 and 0.560 GeV. Vertices with invariant masses outside the range 0.470–0.530 GeV are used as sidebands. A first order polynomial is fitted to the sideband regions, and the number of K^0_S decay candidate vertices is determined by subtracting the fitted background from the total number of vertices with invariant mass in the 0.470–0.560 GeV range. The simulation is normalized such that the number of K^0_S decay candidate vertices at small L_{xy} is the same in data and simulation. The distributions after normalization in 2017 and 2018 data are shown in figure 8. The spread of the ratio of data and simulation, defined as 68% of the size of its envelope, is assigned as the systematic uncertainty, with a magnitude of 10–11%. To confirm that these results are valid for vertices with more than two tracks, a similar study is performed using vertices around b jets, and consistent behavior is observed.

Since the material maps are derived from data, discrepancies may arise because of potential differences in the modeling of detector material between data and simulation. To account for

JHEP05(2026)191

Systematic uncertainty	Magnitude
Background estimate	<2%
Track/vertex reconstruction	10–11%
Material map veto	1–3%
Jet energy scale	2–4%
Jet energy resolution	1–2%
Unclustered energy	1–2%
Pileup	3–4%
Trigger	3%
Scale variations	1–5%
PDF variations	<1%
Integrated luminosity	2–3%
L1 trigger inefficiency	<1%

Table 1. Summary of the systematic uncertainties. The magnitude represents the change in the event yields.

this, a corresponding material map is constructed using simulated events, and the resulting variation in the signal yield is taken as a systematic uncertainty. This uncertainty ranges 1–3%.

The selections on the ISR jet and $p_{\mathrm{T}}^{\mathrm{miss}}$ are affected by the jet energy scale, jet energy resolution, and unclustered energy. The corresponding systematic uncertainties are evaluated by shifting the parameters that describe the mismodeling by one standard deviation. The resulting magnitude is 2–4% for the jet energy scale, 1–2% for the jet energy resolution, and 1–2% for the unclustered energy. The uncertainty in the modeling of the pileup distribution arises from the uncertainty in the total inelastic cross section. It is evaluated from the variation in the reweighted signal event yield when the cross section is varied within its uncertainty [70], resulting in a magnitude of 3–4%. The modeling of $p_{\mathrm{T}}^{\mathrm{miss}}$ trigger efficiency results in a systematic uncertainty of 3%.

The measurement of the integrated luminosity for the 2017 and 2018 data-taking years results in an uncertainty of 2–3% [71, 72]. Variations in the PDFs and the renormalization and factorization scales used in signal simulation lead to changes in the selection efficiencies of the signal models. These uncertainties are estimated by reweighting the simulated signal events according to the variations among different NNPDF replicas [73] and the scale choices. The resulting uncertainties in the selection efficiency are less than 1% from PDFs and 1–5% from the scale variations (up and down by a factor of two, with the two extreme variations excluded). During the 2017 data-taking year, a gradual timing shift in the ECAL was not correctly accounted for in the L1 trigger, resulting in an efficiency drop for events with significant ECAL energy distributed in the high-η region. This effect is simulated and results in a residual uncertainty in the signal yield of less than 1%.

JHEP05(2026)191

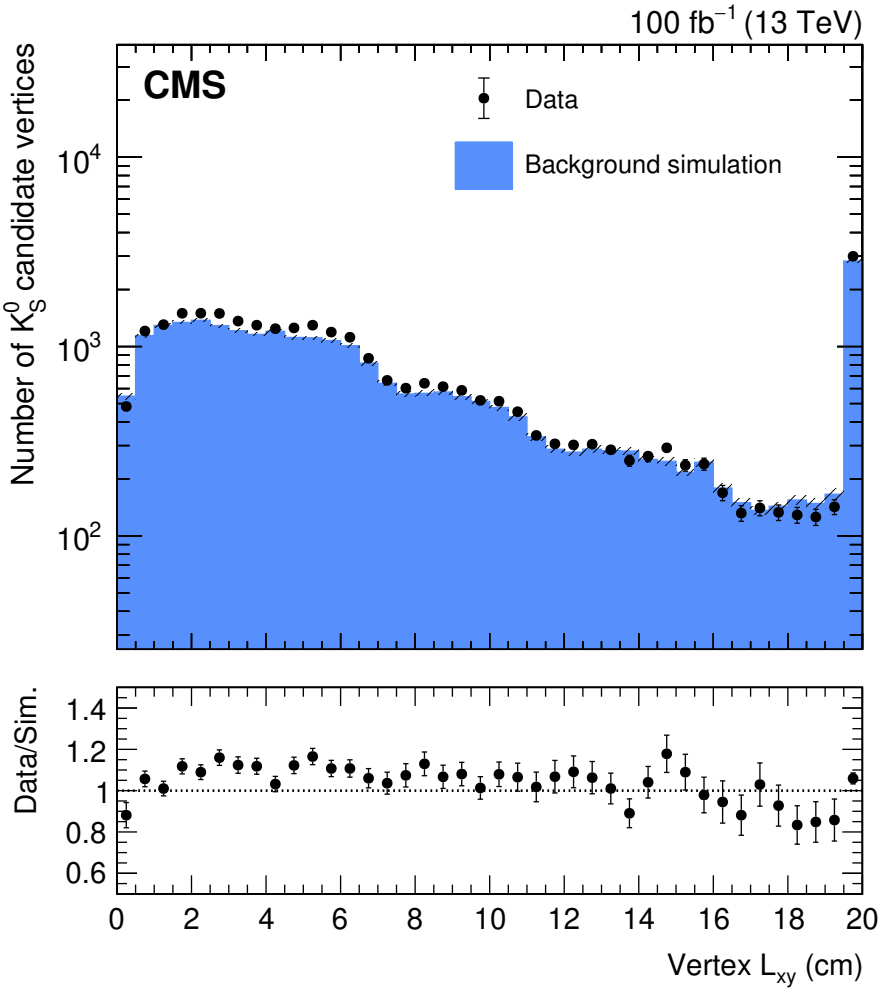

Figure 8. The K^0_S decay candidate vertex L_{xy} distribution compared between data and simulation. The ratios between data and simulation are shown in the lower panel.

7 Results and statistical interpretation

A maximum likelihood fit is performed in all of the regions described in section 5, under the background-only assumption, using the CMS statistical analysis tool Combine [74]. The systematic uncertainties are treated as uncorrelated nuisance parameters in the fit.

For each search plane, the observed data yields and background predictions after the fit are presented in figure 9. The figure also includes the expected yields and their statistical uncertainties from two representative signal models: a $\widetilde{\mathrm{t}}$ NLSP signal model with $m_{\widetilde{\mathrm{t}}} = 1000\,\mathrm{GeV}$, $\Delta m = 20\,\mathrm{GeV}$, and $\mathcal{B} = 100\%$ ($c\tau$ =2.53 mm); and a bino-wino NLSP model with $m_{\mathrm{LLP}} = 400\,\mathrm{GeV}$, $\Delta m = 20\,\mathrm{GeV}$, and $c\tau = 20\,\mathrm{mm}$. The predicted central values are shown along with their associated uncertainties, excluding Poisson statistical uncertainties. Differences between the predicted and observed yields are observed in several regions. In the tight selection plane, regions B and D show predicted yields of 7.7 and 9.2 events, whereas the corresponding observed numbers of events are three and five. In region B of the medium plane, the observed yield of 98 events exceeds the prediction of 78.8. An observed p-value [75]

JHEP05(2026)191

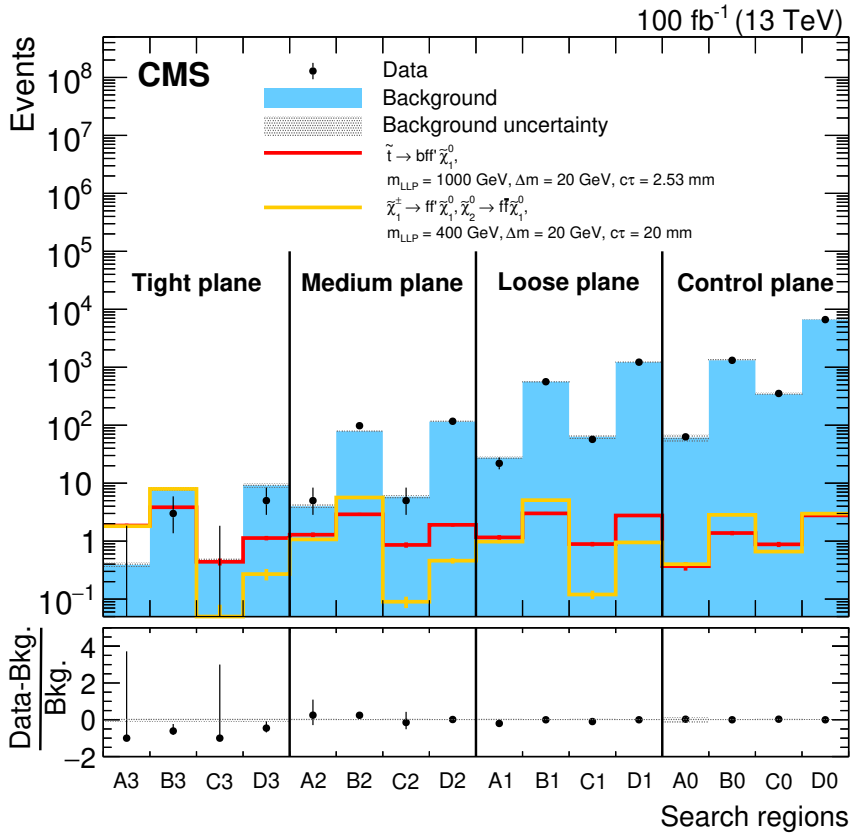

Figure 9. The number of observed and predicted background events after the fit to the regions of the search planes. In addition, two representative signals are shown. The predicted background is shown with its associated uncertainties. The observed data are displayed with the 68% confidence level Poisson confidence intervals. The lower panel shows the fractional difference between the observed data and the predicted background.

of 0.5, obtained from the combined comparison of observed and predicted background yields across all regions, indicates no significant deviation from the background-only hypothesis. Regions A and B in the tight selection plane provide the highest sensitivity for signal models with $c\tau > 1\,\text{mm}$, while regions C and D are more sensitive to models with smaller $c\tau$ values.

To constrain signal model parameters, the 95% confidence level (CL) upper limit on the production cross section for a given assumption of the branching fraction is extracted using the CL_s criterion [74, 76, 77] with the profile likelihood ratio as the test statistic. Data sets from different data-taking years are treated separately and combined during the final fit. The upper limits are compared with the theoretical prediction of the production cross section and uncertainty [78] calculated at NNLO+NNLL precision [54] to exclude regions of the parameter space of the benchmark signal models.

Figures 10 and 11 present the upper limits and exclusion regions for the $\widetilde{\text{t}}$ NLSP model and the bino-wino NLSP model, respectively. For the $\widetilde{\text{t}}$ NLSP model, the limits are shown as functions of Δm and m_LLP under different assumptions of $\mathcal{B}(\widetilde{\text{t}} \to \text{bf}\overline{\text{f}}'\widetilde{\chi}_1^0)$. For the bino-wino NLSP model, they are displayed as functions of the m_LLP and $c\tau$, with different Δm scenarios shown in separate plots. The observed upper limits are lower than the expected

JHEP05(2026)191

ones due to differences between the observed and predicted yields in regions B and D of the tight signal plane.

The search sensitivity depends strongly on the $c\tau$. The optimal sensitivity is achieved for moderate values of $c\tau$ around 10 mm. Sensitivity degrades at low $c\tau$ because of the displacement requirements in track and vertex reconstruction, and at high $c\tau$ because of reduced reconstruction and selection efficiency for highly displaced tracks. Sensitivity also improves with increasing Δm.

In the $\widetilde{\mathrm{t}}$ NLSP model, where $c\tau$ depends on $\mathcal{B}(\widetilde{\mathrm{t}} \to \mathrm{bf}\overline{\mathrm{f}}'\widetilde{\chi}_1^0)$, Δm, and m_{LLP}, the region of highest sensitivity shifts with $\mathcal{B}(\widetilde{\mathrm{t}} \to \mathrm{bf}\overline{\mathrm{f}}'\widetilde{\chi}_1^0)$ because of the change of $c\tau$. Specifically, the value of Δm that corresponds to a $c\tau$ on the order of $\mathcal{O}(10\,\mathrm{mm})$ increases with increasing $\mathcal{B}(\widetilde{\mathrm{t}} \to \mathrm{bf}\overline{\mathrm{f}}'\widetilde{\chi}_1^0)$. In contrast, for the bino-wino NLSP model, where the parameters are uncorrelated, the sensitivity is maximized for large Δm and moderate $c\tau$.

For the $\widetilde{\mathrm{t}}$ NLSP model, the search excludes $\widetilde{\mathrm{t}}$ with masses less than 400–1100 GeV, corresponding to theoretical production cross sections of 2150–3 fb, depending on the Δm and $\mathcal{B}(\widetilde{\mathrm{t}} \to \mathrm{bf}\overline{\mathrm{f}}'\widetilde{\chi}_1^0)$. This parameter space has not been explored by previous searches. For the bino-wino NLSP model, the search excludes NLSPs with masses below 220–550 GeV, corresponding to theoretical production cross sections of 1268–30 fb, depending on the Δm and $c\tau$.

8 Summary

A search for long-lived particles in signatures with displaced vertices with low-momentum tracks, missing transverse momentum, and an initial-state radiation jet has been presented. Proton-proton collision data at a center-of-mass energy of 13 TeV collected by the CMS experiment at the CERN LHC, with a total integrated luminosity of 100 fb^{-1}, are used in the search. Compared with the previous CMS and ATLAS searches using displaced vertices, this search targets vertices with tracks of significantly lower momenta. This search adopts specific supersymmetric (SUSY) coannihilation scenarios as benchmark signal models, characterized by a long-lived next-to-lightest SUSY particle (NLSP) with a mass difference of less than 25 GeV relative to the lightest SUSY particle, assumed to be a bino-like neutralino. In the top squark ($\widetilde{\mathrm{t}}$) NLSP model, the NLSP is a $\widetilde{\mathrm{t}}$, while in the bino-wino NLSP scenario, the mass-degenerate NLSPs are a wino-like long-lived neutralino and a short-lived chargino.

This search reconstructs displaced vertices using a customized algorithm based on the inclusive vertex finder [47]. In addition, the background estimation method using transfer factors allows for targeting multiple signal regions, thus enhancing the search sensitivity.

The search shows good overall agreement between the background predictions and observed event yields across most of the signal regions. The search excludes $\widetilde{\mathrm{t}}$ masses less than 400–1100 GeV and wino-like neutralinos with masses less than 220–550 GeV, depending on the signal parameters. This search is the first at the LHC to demonstrate sensitivity to long-lived particles in compressed-spectrum scenarios using displaced-vertex signatures. It sets the most stringent upper limits to date for the $\widetilde{\mathrm{t}}$ and bino-wino NLSP signal models.

JHEP05(2026)191

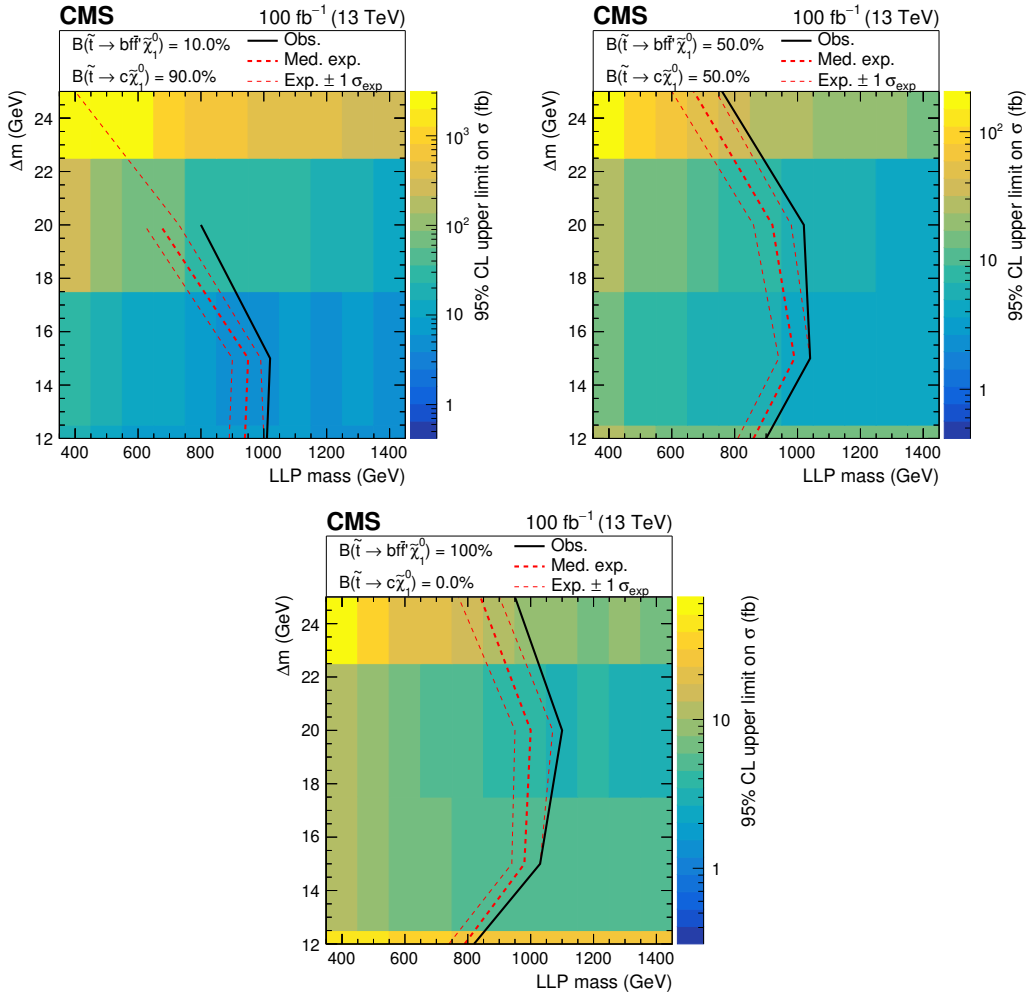

Figure 10. Observed 95% CL upper limits on the $\tilde{t}$ production cross section, as functions of $m_{\tilde{t}}$ and Δm, for $\mathcal{B}(\tilde{t} \to bff'\tilde{\chi}_1^0)$ of 10% (upper left), 50% (upper right), and 100% (lower). The observed (solid black) and expected (dashed red) exclusion curves are overlaid on the plots. The search excludes the region to the left of the exclusion curves. For $\mathcal{B}(\tilde{t} \to bff'\tilde{\chi}_1^0) = 10\%$ (upper left), the exclusion curves terminate at $\Delta m = 20\,\text{GeV}$, as no masses can be excluded at larger mass splittings because of reduced sensitivity in this region.

JHEP05(2026)191

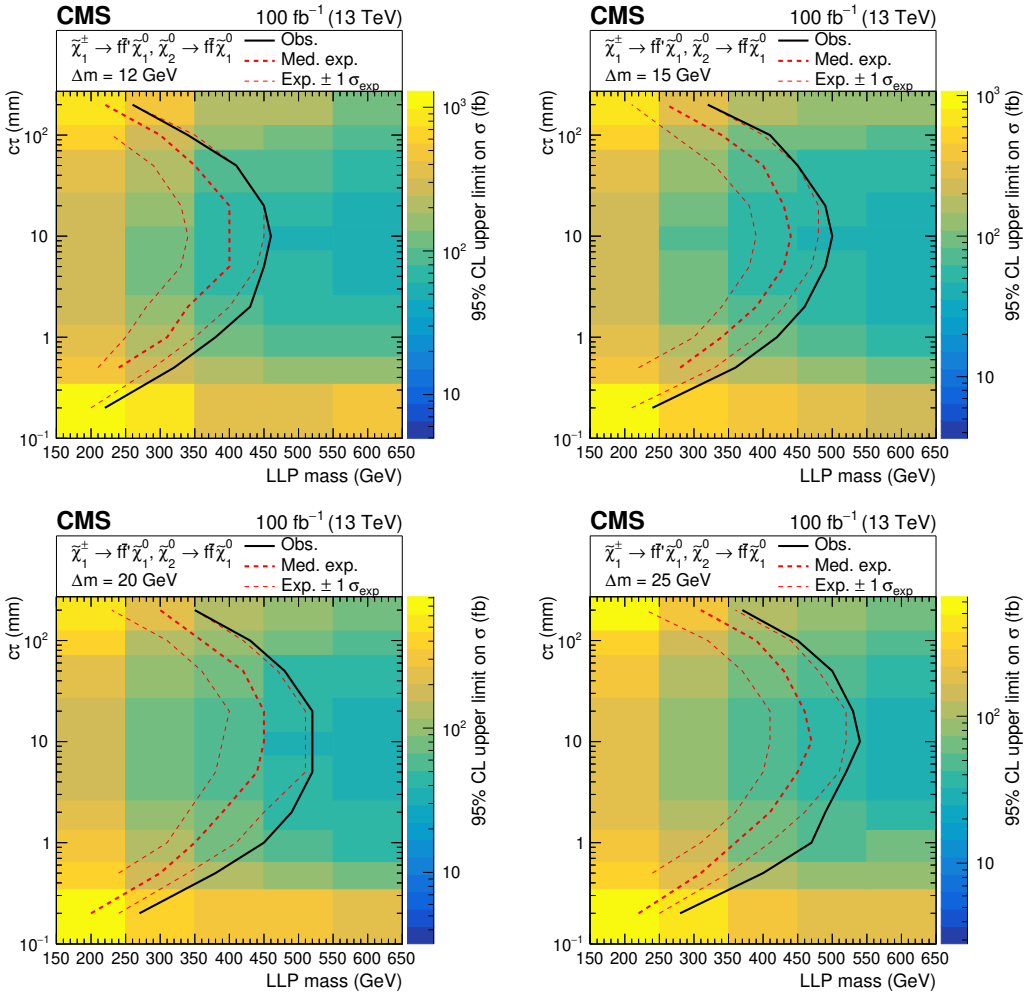

Figure 11. Observed 95% CL upper limits on the production cross section for the bino-wino NLSP model, as functions of m_{LLP} and $c\tau$, for Δm of 12 GeV (upper left), 15 GeV (upper right), 20 GeV (lower left), and 25 GeV (lower right). The observed (solid black) and expected (dashed red) exclusion curves are overlaid on the plots. The search excludes the region to the left of the exclusion curves.

JHEP05(2026)191

Acknowledgments

We congratulate our colleagues in the CERN accelerator departments for the excellent performance of the LHC and thank the technical and administrative staffs at CERN and at other CMS institutes for their contributions to the success of the CMS effort. In addition, we gratefully acknowledge the computing centers and personnel of the Worldwide LHC Computing Grid and other centers for delivering so effectively the computing infrastructure essential to our analyses. Finally, we acknowledge the enduring support for the construction and operation of the LHC, the CMS detector, and the supporting computing infrastructure provided by the following funding agencies: SC (Armenia), BMBWF and FWF (Austria); FNRS and FWO (Belgium); CNPq, CAPES, FAPERJ, FAPERGS, and FAPESP (Brazil); MES and BNSF (Bulgaria); CERN; CAS, MoST, and NSFC (China); MINCIENCIAS (Colombia); MSES and CSF (Croatia); RIF (Cyprus); SENESCYT (Ecuador); ERC PRG, TARISTU24-TK10 and MoER TK202 (Estonia); Academy of Finland, MEC, and HIP (Finland); CEA and CNRS/IN2P3 (France); SRNSF (Georgia); BMFTR, DFG, and HGF (Germany); GSRI (Greece); NKFIH (Hungary); DAE and DST (India); IPM (Iran); SFI (Ireland); INFN (Italy); MSIT and NRF (Republic of Korea); MES (Latvia); LMTLT (Lithuania); MOE and UM (Malaysia); BUAP, CINVESTAV, CONACYT, LNS, SEP, and UASLP-FAI (Mexico); MOS (Montenegro); MBIE (New Zealand); PAEC (Pakistan); MES, NSC, and NAWA (Poland); FCT (Portugal); MESTD (Serbia); MICIU/AEI and PCTI (Spain); MOSTR (Sri Lanka); Swiss Funding Agencies (Switzerland); MST (Taipei); MHESI (Thailand); TUBITAK and TENMAK (Türkiye); NASU (Ukraine); STFC (United Kingdom); DOE and NSF (U.S.A.).

Individuals have received support from the Marie-Curie program and the European Research Council and Horizon 2020 Grant, contract Nos. 675440, 724704, 752730, 758316, 765710, 824093, 101115353, 101002207, 101001205, and COST Action CA16108 (European Union); the Leventis Foundation; the Alfred P. Sloan Foundation; the Alexander von Humboldt Foundation; the Science Committee, project no. 22rl-037 (Armenia); the Fonds pour la Formation à la Recherche dans l'Industrie et dans l'Agriculture (FRIA) and Fonds voor Wetenschappelijk Onderzoek contract No. 1228724N (Belgium); the Beijing Municipal Science & Technology Commission, No. Z191100007219010, the Fundamental Research Funds for the Central Universities, the Ministry of Science and Technology of China under Grant No. 2023YFA1605804, the Natural Science Foundation of China under Grant No. 12061141002, 12535004, and USTC Research Funds of the Double First-Class Initiative No. YD2030002017 (China); the Ministry of Education, Youth and Sports (MEYS) of the Czech Republic; the Shota Rustaveli National Science Foundation, grant FR-22-985 (Georgia); the Deutsche Forschungsgemeinschaft (DFG), among others, under Germany's Excellence Strategy – EXC 2121 "Quantum Universe" – 390833306, and under project number 400140256 – GRK2497; the Hellenic Foundation for Research and Innovation (HFRI), Project Number 2288 (Greece); the Hungarian Academy of Sciences, the New National Excellence Program – ÚNKP, the NKFIH research grants K 131991, K 133046, K 138136, K 143460, K 143477, K 146913, K 146914, K 147048, 2020-2.2.1-ED-2021-00181, TKP2021-NKTA-64, and 2021-4.1.2-NEMZ_KI-2024-00036 (Hungary); the Council of Science and Industrial Research, India; ICSC – National Research Center for High Performance Computing, Big Data and Quantum Computing, FAIR – Future Artificial Intelligence Research, and CUP I53D23001070006 (Mission 4 Component 1),

JHEP05(2026)191

funded by the NextGenerationEU program (Italy); the Latvian Council of Science; the Ministry of Education and Science, project no. 2022/WK/14, and the National Science Center, contracts Opus 2021/41/B/ST2/01369, 2021/43/B/ST2/01552, 2023/49/B/ST2/03273, and the NAWA contract BPN/PPO/2021/1/00011 (Poland); the Fundação para a Ciência e a Tecnologia, grant CEECIND/01334/2018 (Portugal); the National Priorities Research Program by Qatar National Research Fund;h MICIU/AEI/10.13039/501100011033, ERDF/EU, "European Union NextGenerationEU/PRTR", and Programa Severo Ochoa del Principado de Asturias (Spain); the Chulalongkorn Academic into Its 2nd Century Project Advancement Project, the National Science, Research and Innovation Fund program IND_FF_68_369_2300_097, and the Program Management Unit for Human Resources & Institutional Development, Research and Innovation, grant B39G680009 (Thailand); the Kavli Foundation; the Nvidia Corporation; the SuperMicro Corporation; the Welch Foundation, contract C-1845; and the Weston Havens Foundation (U.S.A.).

Data Availability Statement. Release and preservation of data used by the CMS Collaboration as the basis for publications is guided by the CMS data preservation, re-use and open access policy.

Code Availability Statement. The CMS core software is publicly available on GitHub.

References

[1] A. Delgado et al., *The light stop window*, *Eur. Phys. J. C* **73** (2013) 2370 [arXiv:1212.6847] [INSPIRE].

[2] R. Gröber, M.M. Mühlleitner, E. Popenda and A. Wlotzka, *Light Stop Decays: Implications for LHC Searches*, *Eur. Phys. J. C* **75** (2015) 420 [arXiv:1408.4662] [INSPIRE].

[3] N. Nagata, H. Otono and S. Shirai, *Probing Bino-Wino Coannihilation at the LHC*, *JHEP* **10** (2015) 086 [arXiv:1506.08206] [INSPIRE].

[4] G.F. Giudice and A. Romanino, *Split supersymmetry*, *Nucl. Phys. B* **699** (2004) 65 [hep-ph/0406088] [INSPIRE].

[5] J.A.L. Hewett, B. Lillie, M. Masip and T.G. Rizzo, *Signatures of long-lived gluinos in split supersymmetry*, *JHEP* **09** (2004) 070 [hep-ph/0408248] [INSPIRE].

[6] N. Arkani-Hamed, S. Dimopoulos, G.F. Giudice and A. Romanino, *Aspects of split supersymmetry*, *Nucl. Phys. B* **709** (2005) 3 [hep-ph/0409232] [INSPIRE].

[7] P. Gambino, G.F. Giudice and P. Slavich, *Gluino decays in split supersymmetry*, *Nucl. Phys. B* **726** (2005) 35 [hep-ph/0506214] [INSPIRE].

[8] A. Arvanitaki, N. Craig, S. Dimopoulos and G. Villadoro, *Mini-Split*, *JHEP* **02** (2013) 126 [arXiv:1210.0555] [INSPIRE].

[9] N. Arkani-Hamed et al., *Simply Unnatural Supersymmetry*, arXiv:1212.6971 [INSPIRE].

JHEP05(2026)191

[10] J.J. Fan, M. Reece and J.T. Ruderman, *Stealth Supersymmetry*, *JHEP* **11** (2011) 012 [arXiv:1105.5135] [INSPIRE].

[11] J.J. Fan, M. Reece and J.T. Ruderman, *A Stealth Supersymmetry Sampler*, *JHEP* **07** (2012) 196 [arXiv:1201.4875] [INSPIRE].

[12] G.F. Giudice and R. Rattazzi, *Theories with gauge mediated supersymmetry breaking*, *Phys. Rept.* **322** (1999) 419 [hep-ph/9801271] [INSPIRE].

[13] P. Meade, N. Seiberg and D. Shih, *General Gauge Mediation*, *Prog. Theor. Phys. Suppl.* **177** (2009) 143 [arXiv:0801.3278] [INSPIRE].

[14] M. Buican, P. Meade, N. Seiberg and D. Shih, *Exploring General Gauge Mediation*, *JHEP* **03** (2009) 016 [arXiv:0812.3668] [INSPIRE].

[15] M.J. Strassler and K.M. Zurek, *Echoes of a hidden valley at hadron colliders*, *Phys. Lett. B* **651** (2007) 374 [hep-ph/0604261] [INSPIRE].

[16] M.J. Strassler and K.M. Zurek, *Discovering the Higgs through highly-displaced vertices*, *Phys. Lett. B* **661** (2008) 263 [hep-ph/0605193] [INSPIRE].

[17] T. Han, Z. Si, K.M. Zurek and M.J. Strassler, *Phenomenology of hidden valleys at hadron colliders*, *JHEP* **07** (2008) 008 [arXiv:0712.2041] [INSPIRE].

[18] ATLAS collaboration, *Search for long-lived, massive particles in events with displaced vertices and missing transverse momentum in* $\sqrt{s} = 13$ *TeV pp collisions with the ATLAS detector*, *Phys. Rev. D* **97** (2018) 052012 [arXiv:1710.04901] [INSPIRE].

[19] ATLAS collaboration, *Search for long-lived, massive particles in events with a displaced vertex and a muon with large impact parameter in pp collisions at* $\sqrt{s} = 13$ *TeV with the ATLAS detector*, *Phys. Rev. D* **102** (2020) 032006 [arXiv:2003.11956] [INSPIRE].

[20] CMS collaboration, *Search for long-lived particles decaying to jets with displaced vertices in proton-proton collisions at* $\sqrt{s} = 13$ *TeV*, *Phys. Rev. D* **104** (2021) 052011 [arXiv:2104.13474] [INSPIRE].

[21] CMS collaboration, *Search for long-lived particles using displaced jets in proton-proton collisions at* $\sqrt{s} = 13$ *TeV*, *Phys. Rev. D* **104** (2021) 012015 [arXiv:2012.01581] [INSPIRE].

[22] ATLAS collaboration, *Search for long-lived, massive particles in events with displaced vertices and multiple jets in pp collisions at* $\sqrt{s} = 13$ *TeV with the ATLAS detector*, *JHEP* **06** (2023) 200 [arXiv:2301.13866] [INSPIRE].

[23] CMS collaboration, *Search for long-lived particles using displaced vertices and missing transverse momentum in proton-proton collisions at* $\sqrt{s} = 13$ *TeV*, *Phys. Rev. D* **109** (2024) 112005 [arXiv:2402.15804] [INSPIRE].

[24] CMS collaboration, *Search for light long-lived particles decaying to displaced jets in proton-proton collisions at* $\sqrt{s} = 13.6$ *TeV*, *Rept. Prog. Phys.* **88** (2025) 037801 [arXiv:2409.10806] [INSPIRE].

[25] B. Cardwell, *Search for displaced leptons in proton-proton collisions at* $\sqrt{s} = 13$ *TeV*, Ph.D. Thesis, Ohio State University, U.S.A. (2021).

[26] A. Djouadi, M. Drees, P. Fileviez Perez and M. Mühlleitner, *Loop induced Higgs and Z boson couplings to neutralinos and implications for collider and dark matter searches*, *Phys. Rev. D* **65** (2002) 075016 [hep-ph/0109283] [INSPIRE].

[27] ATLAS collaboration, *Statistical Combination of ATLAS Run 2 Searches for Charginos and Neutralinos at the LHC*, *Phys. Rev. Lett.* **133** (2024) 031802 [arXiv:2402.08347] [INSPIRE].

JHEP05(2026)191

[28] CMS collaboration, *Combined search for electroweak production of winos, binos, higgsinos, and sleptons in proton-proton collisions at* $\sqrt{s} = 13, TeV$, *Phys. Rev. D* **109** (2024) 112001 [arXiv:2402.01888] [INSPIRE].

[29] *HEPData record for this analysis*, (2024), DOI:10.17182/hepdata.166009.

[30] CMS collaboration, *The CMS Experiment at the CERN LHC*, 2008 *JINST* **3** S08004 [INSPIRE].

[31] CMS collaboration, *Development of the CMS detector for the CERN LHC Run 3*, 2024 *JINST* **19** P05064 [arXiv:2309.05466] [INSPIRE].

[32] CMS collaboration, *The CMS trigger system*, 2017 *JINST* **12** P01020 [arXiv:1609.02366] [INSPIRE].

[33] CMS collaboration, *Performance of the CMS Level-1 trigger in proton-proton collisions at* $\sqrt{s} = 13$ *TeV*, 2020 *JINST* **15** P10017 [arXiv:2006.10165] [INSPIRE].

[34] CMS collaboration, *Performance of the CMS high-level trigger during LHC Run 2*, 2024 *JINST* **19** P11021 [arXiv:2410.17038] [INSPIRE].

[35] CMS collaboration, *Electron and photon reconstruction and identification with the CMS experiment at the CERN LHC*, 2021 *JINST* **16** P05014 [arXiv:2012.06888] [INSPIRE].

[36] CMS collaboration, *Performance of the CMS muon detector and muon reconstruction with proton-proton collisions at* $\sqrt{s} = 13$ *TeV*, 2018 *JINST* **13** P06015 [arXiv:1804.04528] [INSPIRE].

[37] CMS collaboration, *Description and Performance of Track and Primary-Vertex Reconstruction with the CMS Tracker*, 2014 *JINST* **9** P10009 [arXiv:1405.6569] [INSPIRE].

[38] CMS TRACKER GROUP collaboration, *The CMS Phase-1 Pixel Detector Upgrade*, 2021 *JINST* **16** P02027 [arXiv:2012.14304] [INSPIRE].

[39] CMS collaboration, *Track impact parameter resolution for the full pseudo rapidity coverage in the 2017 dataset with the CMS Phase-1 Pixel detector*, CMS Detector Performance Summary CMS-DP-2020-049 (2020).

[40] CMS collaboration, *Particle-flow reconstruction and global event description with the CMS detector*, 2017 *JINST* **12** P10003 [arXiv:1706.04965] [INSPIRE].

[41] D. Contardo et al., *Technical Proposal for the Phase-II Upgrade of the CMS Detector*, CERN-LHCC-2015-010 (2015) [DOI:10.17181/CERN.VU8I.D59J] [INSPIRE].

[42] M. Cacciari, G.P. Salam and G. Soyez, *The anti-*k_t *jet clustering algorithm*, *JHEP* **04** (2008) 063 [arXiv:0802.1189] [INSPIRE].

[43] M. Cacciari, G.P. Salam and G. Soyez, *FastJet User Manual*, *Eur. Phys. J. C* **72** (2012) 1896 [arXiv:1111.6097] [INSPIRE].

[44] CMS collaboration, *Pileup mitigation at CMS in 13 TeV data*, 2020 *JINST* **15** P09018 [arXiv:2003.00503] [INSPIRE].

[45] CMS collaboration, *Jet energy scale and resolution in the CMS experiment in pp collisions at 8 TeV*, 2017 *JINST* **12** P02014 [arXiv:1607.03663] [INSPIRE].

[46] CMS collaboration, *Jet algorithms performance in 13 TeV data*, CMS-PAS-JME-16-003 (2017) [INSPIRE].

[47] CMS collaboration, *Identification of heavy-flavour jets with the CMS detector in pp collisions at 13 TeV*, 2018 *JINST* **13** P05011 [arXiv:1712.07158] [INSPIRE].

[48] E. Bols et al., *Jet Flavour Classification Using DeepJet*, 2020 *JINST* **15** P12012 [arXiv:2008.10519] [INSPIRE].

JHEP05(2026)191

[49] CMS collaboration, *Performance summary of AK4 jet b tagging with data from proton-proton collisions at 13 TeV with the CMS detector*, CMS Detector Performance Summary CMS-DP-2023-005 (2023).

[50] CMS collaboration, *Performance of missing transverse momentum reconstruction in proton-proton collisions at $\sqrt{s} = 13$ TeV using the CMS detector*, 2019 *JINST* **14** P07004 [arXiv:1903.06078] [INSPIRE].

[51] CMS collaboration, *Performance of reconstruction and identification of τ leptons decaying to hadrons and ν_τ in pp collisions at $\sqrt{s} = 13$ TeV*, 2018 *JINST* **13** P10005 [arXiv:1809.02816] [INSPIRE].

[52] J. Alwall et al., *The automated computation of tree-level and next-to-leading order differential cross sections, and their matching to parton shower simulations*, *JHEP* **07** (2014) 079 [arXiv:1405.0301] [INSPIRE].

[53] J. Alwall et al., *Comparative study of various algorithms for the merging of parton showers and matrix elements in hadronic collisions*, *Eur. Phys. J. C* **53** (2008) 473 [arXiv:0706.2569] [INSPIRE].

[54] W. Beenakker et al., *NNLL-fast: predictions for coloured supersymmetric particle production at the LHC with threshold and Coulomb resummation*, *JHEP* **12** (2016) 133 [arXiv:1607.07741] [INSPIRE].

[55] A.C. Kraan, *Interactions of heavy stable hadronizing particles*, *Eur. Phys. J. C* **37** (2004) 91 [hep-ex/0404001] [INSPIRE].

[56] R. Mackeprang and A. Rizzi, *Interactions of Coloured Heavy Stable Particles in Matter*, *Eur. Phys. J. C* **50** (2007) 353 [hep-ph/0612161] [INSPIRE].

[57] R. Frederix and S. Frixione, *Merging meets matching in MC@NLO*, *JHEP* **12** (2012) 061 [arXiv:1209.6215] [INSPIRE].

[58] P. Nason, *A new method for combining NLO QCD with shower Monte Carlo algorithms*, *JHEP* **11** (2004) 040 [hep-ph/0409146] [INSPIRE].

[59] S. Frixione, P. Nason and C. Oleari, *Matching NLO QCD computations with Parton Shower simulations: the POWHEG method*, *JHEP* **11** (2007) 070 [arXiv:0709.2092] [INSPIRE].

[60] S. Alioli, P. Nason, C. Oleari and E. Re, *NLO single-top production matched with shower in POWHEG: s- and t-channel contributions*, *JHEP* **09** (2009) 111 [*Erratum ibid.* **02** (2010) 011] [arXiv:0907.4076] [INSPIRE].

[61] S. Alioli, P. Nason, C. Oleari and E. Re, *A general framework for implementing NLO calculations in shower Monte Carlo programs: the POWHEG BOX*, *JHEP* **06** (2010) 043 [arXiv:1002.2581] [INSPIRE].

[62] E. Re, *Single-top Wt-channel production matched with parton showers using the POWHEG method*, *Eur. Phys. J. C* **71** (2011) 1547 [arXiv:1009.2450] [INSPIRE].

[63] T. Sjöstrand et al., *An introduction to PYTHIA 8.2*, *Comput. Phys. Commun.* **191** (2015) 159 [arXiv:1410.3012] [INSPIRE].

[64] NNPDF collaboration, *Parton distributions for the LHC Run II*, *JHEP* **04** (2015) 040 [arXiv:1410.8849] [INSPIRE].

[65] NNPDF collaboration, *Parton distributions from high-precision collider data*, *Eur. Phys. J. C* **77** (2017) 663 [arXiv:1706.00428] [INSPIRE].

JHEP05(2026)191

[66] CMS collaboration, *Extraction and validation of a new set of CMS PYTHIA8 tunes from underlying-event measurements*, *Eur. Phys. J. C* **80** (2020) 4 [arXiv:1903.12179] [INSPIRE].

[67] GEANT4 collaboration, *GEANT4 — A Simulation Toolkit*, *Nucl. Instrum. Meth. A* **506** (2003) 250 [INSPIRE].

[68] J. D'Hondt, P. Vanlaer, R. Fruhwirth and W. Waltenberger, *Sensitivity of robust vertex fitting algorithms*, *IEEE Trans. Nucl. Sci.* **51** (2004) 2037 [INSPIRE].

[69] CMS collaboration, *Displaced tracking and vertexing calibration using neutral K mesons*, CMS Detector Performance Summary CMS-DP-2024-010 (2024).

[70] CMS collaboration, *Measurement of the inelastic proton-proton cross section at* $\sqrt{s} = 13$ *TeV*, *JHEP* **07** (2018) 161 [arXiv:1802.02613] [INSPIRE].

[71] CMS collaboration, *CMS luminosity measurement for the 2017 data-taking period at* $\sqrt{s} = 13$ *TeV*, CMS-PAS-LUM-17-004 (2018) [INSPIRE].

[72] CMS collaboration, *CMS luminosity measurement for the 2018 data-taking period at* $\sqrt{s} = 13$ *TeV*, CMS-PAS-LUM-18-002 (2019) [INSPIRE].

[73] J. Butterworth et al., *PDF4LHC recommendations for LHC Run II*, *J. Phys. G* **43** (2016) 023001 [arXiv:1510.03865] [INSPIRE].

[74] CMS collaboration, *The CMS Statistical Analysis and Combination Tool: Combine*, *Comput. Softw. Big Sci.* **8** (2024) 19 [arXiv:2404.06614] [INSPIRE].

[75] R.D. Cousins, *Lectures on Statistics in Theory: Prelude to Statistics in Practice*, arXiv:1807.05996 [INSPIRE].

[76] T. Junk, *Confidence level computation for combining searches with small statistics*, *Nucl. Instrum. Meth. A* **434** (1999) 435 [hep-ex/9902006] [INSPIRE].

[77] A.L. Read, *Presentation of search results: The* CL_s *technique*, *J. Phys. G* **28** (2002) 2693 [INSPIRE].

[78] C. Borschensky et al., *Squark and gluino production cross sections in pp collisions at* $\sqrt{s} = 13$, 14, 33 *and* 100 *TeV*, *Eur. Phys. J. C* **74** (2014) 3174 [arXiv:1407.5066] [INSPIRE].

JHEP05(2026)191

The CMS collaboration

A. Hayrapetyan[1], V. Makarenko[1], A. Tumasyan[1,a], W. Adam[2], J.W. Andrejkovic[2], L. Benato[2], T. Bergauer[2], M. Dragicevic[2], C. Giordano[2], A.K. Güven[2], P.S. Hussain[2], M. Jeitler[2,b], N. Krammer[2], A. Li[2], D. Liko[2], M. Matthewman[2], I. Mikulec[2], J. Schieck[2,b], D. Schwarz[2], R. Schöfbeck[2,b], M. Shooshtari[2], M. Sonawane[2], W. Waltenberger[2], C.-E. Wulz[2,b], T. Janssen[3], H. Kwon[3], D. Ocampo Henao[3], T. Van Laer[3], P. Van Mechelen[3], J. Bierkens[4], N. Breugelmans[4], J. D'Hondt[4], S. Dansana[4], A. De Moor[4], M. Delcourt[4], F. Heyen[4], Y. Hong[4], P. Kashko[4], S. Lowette[4], I. Makarenko[4], D. Müller[4], J. Song[4], S. Tavernier[4], M. Tytgat[4,c], G.P. Van Onsem[4], S. Van Putte[4], D. Vannerom[4], B. Bilin[5], B. Clerbaux[5], A.K. Das[5], I. De Bruyn[5], G. De Lentdecker[5], H. Evard[5], L. Favart[5], P. Gianneios[5], A. Khalilzadeh[5], F.A. Khan[5], A. Malara[5], M.A. Shahzad[5], L. Thomas[5], M. Vanden Bemden[5], C. Vander Velde[5], P. Vanlaer[5], F. Zhang[5], M. De Coen[6], D. Dobur[6], G. Gokbulut[6], J. Knolle[6], D. Marckx[6], K. Skovpen[6], A.M. Tomaru[6], N. Van Den Bossche[6], J. van der Linden[6], J. Vandenbroeck[6], L. Wezenbeek[6], S. Bein[7], A. Benecke[7], A. Bethani[7], G. Bruno[7], A. Cappati[7], J. De Favereau De Jeneret[7], C. Delaere[7], A. Giammanco[7], A.O. Guzel[7], V. Lemaitre[7], J. Lidrych[7], P. Malek[7], P. Mastrapasqua[7], S. Turkcapar[7], G.A. Alves[8], M. Barroso Ferreira Filho[8], E. Coelho[8], C. Hensel[8], T. Menezes De Oliveira[8], C. Mora Herrera[8], P. Rebello Teles[8], M. Soeiro[8], E.J. Tonelli Manganote[8,d], A. Vilela Pereira[8,e], W.L. Aldá Júnior[9], H. Brandao Malbouisson[9], W. Carvalho[9], J. Chinellato[9,f], M. Costa Reis[9], E.M. Da Costa[9], G.G. Da Silveira[9,g], D. De Jesus Damiao[9], S. Fonseca De Souza[9], R. Gomes De Souza[9], S. S. Jesus[9], T. Laux Kuhn[9,g], M. Macedo[9], K. Mota Amarilo[9], L. Mundim[9], H. Nogima[9], J.P. Pinheiro[9], A. Santoro[9], A. Sznajder[9], M. Thiel[9], F. Torres Da Silva De Araujo[9,h], C.A. Bernardes[10,g], F. Damas[10], E.M. Gregores[10], B. Lopes Da Costa[10], I. Maietto Silverio[10], P.G. Mercadante[10], S.F. Novaes[10], B. Orzari[10], Sandra S. Padula[10], V. Scheurer[10], T.R. Fernandez Perez Tomei[10], A. Aleksandrov[11], G. Antchev[11], P. Danev[11], R. Hadjiiska[11], P. Iaydjiev[11], M. Shopova[11], G. Sultanov[11], A. Dimitrov[12], L. Litov[12], B. Pavlov[12], P. Petkov[12], A. Petrov[12], S. Keshri[13], D. Laroze[13], S. Thakur[13], W. Brooks[14], T. Cheng[15], T. Javaid[15], L. Wang[15], L. Yuan[15], Z. Hu[16], Z. Liang[16], J. Liu[16], X. Wang[16], H. Yang[16], G.M. Chen[17,i], H.S. Chen[17,i], M. Chen[17,i], Y. Chen[17], Q. Hou[17], X. Hou[17], F. Iemmi[17], C.H. Jiang[17], A. Kapoor[17,j], H. Liao[17], G. Liu[17], Z.-A. Liu[17,k], J.N. Song[17,k], S. Song[17], J. Tao[17], C. Wang[17,i], J. Wang[17], H. Zhang[17], J. Zhao[17], A. Agapitos[18], Y. Ban[18], A. Carvalho Antunes De Oliveira[18], S. Deng[18], B. Guo[18], Q. Guo[18], C. Jiang[18], A. Levin[18], C. Li[18], Q. Li[18], Y. Mao[18], S. Qian[18], S.J. Qian[18], X. Qin[18], C. Quaranta[18], X. Sun[18], D. Wang[18], J. Wang[18], M. Zhang[18], Y. Zhao[18], C. Zhou[18], S. Yang[19], Z. You[20], K. Jaffel[21], N. Lu[21], G. Bauer[22,l,m], Z. Cui[22,m], B. Li[22,n], H. Wang[22], K. Yi[22,o], J. Zhang[22], Y. Li[23], Z. Lin[24], C. Lu[24], M. Xiao[24,p], C. Avila[25], D.A. Barbosa Trujillo[25], A. Cabrera[25], C. Florez[25], J. Fraga[25], J.A. Reyes Vega[25], C. Rendón[26], M. Rodriguez[26], A.A. Ruales Barbosa[26], J.D. Ruiz Alvarez[26], N. Godinovic[27], D. Lelas[27], A. Sculac[27], M. Kovac[28], A. Petkovic[28], T. Sculac[28], P. Bargassa[29], V. Brigljevic[29], B.K. Chitroda[29], D. Ferencek[29], K. Jakovcic[29], A. Starodumov[29], T. Susa[29], A. Attikis[30], K. Christoforou[30],

JHEP05(2026)191

C. Leonidou[30], C. Nicolaou[30], L. Paizanos[30], F. Ptochos[30], P.A. Razis[30], H. Rykaczewski[30], H. Saka[30], A. Stepennov[30], M. Finger[31,†], M. Finger Jr.[31], E. Ayala[32], E. Carrera Jarrin[33], S. Elgammal[34,q], A. Ellithi Kamel[34,r], A. Hussein[35], H. Mohammed[35], K. Ehataht[36], M. Kadastik[36], T. Lange[36], C. Nielsen[36], J. Pata[36], M. Raidal[36], N. Seeba[36], L. Tani[36], E. Brücken[37], A. Milieva[37], K. Osterberg[37], M. Voutilainen[37], F. Garcia[38], P. Inkaew[38], K.T.S. Kallonen[38], R. Kumar Verma[38], T. Lampén[38], K. Lassila-Perini[38], B. Lehtela[38], S. Lehti[38], T. Lindén[38], N.R. Mancilla Xinto[38], M. Myllymäki[38], M.m. Rantanen[38], S. Saariokari[38], N.T. Toikka[38], J. Tuominiemi[38], N. Bin Norjoharuddeen[39], H. Kirschenmann[39], P. Luukka[39], H. Petrow[39], M. Besancon[40], F. Couderc[40], M. Dejardin[40], D. Denegri[40], P. Devouge[40], J.L. Faure[40], F. Ferri[40], P. Gaigne[40], S. Ganjour[40], P. Gras[40], G. Hamel de Monchenault[40], M. Kumar[40], V. Lohezic[40], Y. Maidannyk[40], J. Malcles[40], F. Orlandi[40], L. Portales[40], S. Ronchi[40], M.Ö. Sahin[40], A. Savoy-Navarro[40,s], P. Simkina[40], M. Titov[40], M. Tornago[40], R. Amella Ranz[41], F. Beaudette[41], G. Boldrini[41], P. Busson[41], C. Charlot[41], M. Chiusi[41], T.D. Cuisset[41], O. Davignon[41], A. De Wit[41], T. Debnath[41], I.T. Ehle[41], S. Ghosh[41], A. Gilbert[41], R. Granier de Cassagnac[41], L. Kalipoliti[41], M. Manoni[41], M. Nguyen[41], S. Obraztsov[41], C. Ochando[41], R. Salerno[41], J.B. Sauvan[41], Y. Sirois[41], G. Sokmen[41], L. Urda Gómez[41], A. Zabi[41], A. Zghiche[41], J.-L. Agram[42,t], J. Andrea[42], D. Bloch[42], J.-M. Brom[42], E.C. Chabert[42], C. Collard[42], G. Coulon[42], S. Falke[42], U. Goerlach[42], R. Haeberle[42], A.-C. Le Bihan[42], M. Meena[42], O. Poncet[42], G. Saha[42], P. Vaucelle[42], A. Di Florio[43], D. Amram[44], S. Beauceron[44], B. Blancon[44], G. Boudoul[44], N. Chanon[44], D. Contardo[44], P. Depasse[44], H. El Mamouni[44], J. Fay[44], S. Gascon[44], M. Gouzevitch[44], C. Greenberg[44], G. Grenier[44], B. Ille[44], E. Jourd'Huy[44], M. Lethuillier[44], B. Massoteau[44], L. Mirabito[44], A. Purohit[44], M. Vander Donckt[44], J. Xiao[44], I. Lomidze[45], T. Toriashvili[45,u], Z. Tsamalaidze[45,v], V. Botta[46], S. Consuegra Rodríguez[46], L. Feld[46], K. Klein[46], M. Lipinski[46], D. Meuser[46], P. Nattland[46], V. Oppenländer[46], A. Pauls[46], D. Pérez Adán[46], N. Röwert[46], M. Teroerde[46], C. Daumann[47], S. Diekmann[47], A. Dodonova[47], N. Eich[47], D. Eliseev[47], F. Engelke[47], J. Erdmann[47], M. Erdmann[47], B. Fischer[47], T. Hebbeker[47], K. Hoepfner[47], F. Ivone[47], A. Jung[47], N. Kumar[47], M.y. Lee[47], F. Mausolf[47], M. Merschmeyer[47], A. Meyer[47], F. Nowotny[47], A. Pozdnyakov[47], W. Redjeb[47], H. Reithler[47], U. Sarkar[47], V. Sarkisovi[47], A. Schmidt[47], C. Seth[47], A. Sharma[47], J.L. Spah[47], V. Vaulin[47], S. Zaleski[47], M.R. Beckers[48], C. Dziwok[48], G. Flügge[48], N. Hoeflich[48], T. Kress[48], A. Nowack[48], O. Pooth[48], A. Stahl[48], A. Zotz[48], H. Aarup Petersen[49], A. Abel[49], M. Aldaya Martin[49], J. Alimena[49], S. Amoroso[49], Y. An[49], I. Andreev[49], J. Bach[49], S. Baxter[49], M. Bayatmakou[49], H. Becerril Gonzalez[49], O. Behnke[49], A. Belvedere[49], F. Blekman[49,w], K. Borras[49,x], A. Campbell[49], S. Chatterjee[49], L.X. Coll Saravia[49], G. Eckerlin[49], D. Eckstein[49], E. Gallo[49,w], A. Geiser[49], V. Guglielmi[49], M. Guthoff[49], A. Hinzmann[49], L. Jeppe[49], M. Kasemann[49], C. Kleinwort[49], R. Kogler[49], M. Komm[49], D. Krücker[49], W. Lange[49], D. Leyva Pernia[49], K.-Y. Lin[49], K. Lipka[49,y], W. Lohmann[49,z], J. Malvaso[49], R. Mankel[49], I.-A. Melzer-Pellmann[49], M. Mendizabal Morentin[49], A.B. Meyer[49], G. Milella[49], K. Moral Figueroa[49], A. Mussgiller[49], L.P. Nair[49], J. Niedziela[49], A. Nürnberg[49], J. Park[49], E. Ranken[49], A. Raspereza[49], D. Rastorguev[49], L. Rygaard[49],

JHEP05(2026)191

M. Scham[49,aa,ab], S. Schnake[49,x], C. Schwanenberger[49,w], P. Schütze[49], D. Selivanova[49], K. Sharko[49], M. Shchedrolosiev[49], D. Stafford[49], M. Torkian[49], F. Vazzoler[49], A. Ventura Barroso[49], R. Walsh[49], D. Wang[49], Q. Wang[49], K. Wichmann[49], L. Wiens[49,x], C. Wissing[49], Y. Yang[49], S. Zakharov[49], A. Zimermmane Castro Santos[49], A.R. Alves Andrade[50], M. Antonello[50], S. Bollweg[50], M. Bonanomi[50], K. El Morabit[50], Y. Fischer[50], M. Frahm[50], E. Garutti[50], A. Grohsjean[50], A.A. Guvenli[50], J. Haller[50], D. Hundhausen[50], G. Kasieczka[50], P. Keicher[50], R. Klanner[50], W. Korcari[50], T. Kramer[50], C.c. Kuo[50], F. Labe[50], J. Lange[50], A. Lobanov[50], L. Moureaux[50], A. Nigamova[50], K. Nikolopoulos[50], A. Paasch[50], K.J. Pena Rodriguez[50], N. Prouvost[50], B. Raciti[50], M. Rieger[50], D. Savoiu[50], P. Schleper[50], M. Schröder[50], J. Schwandt[50], M. Sommerhalder[50], H. Stadie[50], G. Steinbrück[50], R. Ward[50], B. Wiederspan[50], M. Wolf[50], S. Brommer[51], E. Butz[51], Y.M. Chen[51], T. Chwalek[51], A. Dierlamm[51], G.G. Dincer[51], U. Elicabuk[51], N. Faltermann[51], M. Giffels[51], A. Gottmann[51], F. Hartmann[51,ac], M. Horzela[51], F. Hummer[51], U. Husemann[51], J. Kieseler[51], M. Klute[51], R. Kunnilan Muhammed Rafeek[51], O. Lavoryk[51], J.M. Lawhorn[51], A. Lintuluoto[51], S. Maier[51], M. Mormile[51], Th. Müller[51], E. Pfeffer[51], M. Presilla[51], G. Quast[51], K. Rabbertz[51], B. Regnery[51], R. Schmieder[51], N. Shadskiy[51], I. Shvetsov[51], H.J. Simonis[51], L. Sowa[51], L. Stockmeier[51], K. Tauqeer[51], M. Toms[51], B. Topko[51], N. Trevisani[51], C. Verstege[51], T. Voigtländer[51], R.F. Von Cube[51], J. Von Den Driesch[51], M. Wassmer[51], R. Wolf[51], W.D. Zeuner[51], X. Zuo[51], G. Anagnostou[52], G. Daskalakis[52], A. Kyriakis[52], G. Melachroinos[53], Z. Painesis[53], I. Paraskevas[53], N. Saoulidou[53], K. Theofilatos[53], E. Tziaferi[53], E. Tzovara[53], K. Vellidis[53], I. Zisopoulos[53], T. Chatzistavrou[54], G. Karapostoli[54], K. Kousouris[54], E. Siamarkou[54], G. Tsipolitis[54], I. Bestintzanos[55], I. Evangelou[55], C. Foudas[55], P. Katsoulis[55], P. Kokkas[55], P.G. Kosmoglou Kioseoglou[55], N. Manthos[55], I. Papadopoulos[55], J. Strologas[55], D. Druzhkin[56], C. Hajdu[56], D. Horvath[56,ad,ae], K. Márton[56], A.J. Rádl[56,af], F. Sikler[56], V. Veszpremi[56], M. Csanád[57], K. Farkas[57], A. Fehérkuti[57,ag], M.M.A. Gadallah[57,ah], Á. Kadlecsik[57], M. León Coello[57], G. Pásztor[57], G.I. Veres[57], B. Ujvari[58], G. Zilizi[58], G. Bencze[59], S. Czellar[59], J. Molnar[59], Z. Szillasi[59], T. Csorgo[60,ag], F. Nemes[60,ag], T. Novak[60], I. Szanyi[60,ai], S. Bansal[61], S.B. Beri[61], V. Bhatnagar[61], G. Chaudhary[61], S. Chauhan[61], N. Dhingra[61,aj], A. Kaur[61], A. Kaur[61], H. Kaur[61], M. Kaur[61], S. Kumar[61], T. Sheokand[61], J.B. Singh[61], A. Singla[61], A. Bhardwaj[62], A. Chhetri[62], B.C. Choudhary[62], A. Kumar[62], A. Kumar[62], M. Naimuddin[62], S. Phor[62], K. Ranjan[62], M.K. Saini[62], S. Acharya[63,ak], B. Gomber[63], B. Sahu[63,ak], S. Mukherjee[64], S. Bhattacharya[65], S. Das Gupta[65], S. Dutta[65], S. Dutta[65], S. Sarkar[65], M.M. Ameen[66], P.K. Behera[66], S. Chatterjee[66], G. Dash[66], A. Dattamunsi[66], P. Jana[66], P. Kalbhor[66], S. Kamble[66], J.R. Komaragiri[66,al], T. Mishra[66], P.R. Pujahari[66], A.K. Sikdar[66], R.K. Singh[66], P. Verma[66], S. Verma[66], A. Vijay[66], B.K. Sirasva[67], L. Bhatt[68], S. Dugad[68], G.B. Mohanty[68], M. Shelake[68], P. Suryadevara[68], A. Bala[69], S. Banerjee[69], S. Barman[69,am], R.M. Chatterjee[69], M. Guchait[69], Sh. Jain[69], A. Jaiswal[69], B.M. Joshi[69], S. Kumar[69], M. Maity[69,am], G. Majumder[69], K. Mazumdar[69], S. Parolia[69], R. Saxena[69], A. Thachayath[69], S. Bahinipati[70,an], D. Maity[70,ao], P. Mal[70], K. Naskar[70,ao], A. Nayak[70,ao], S. Nayak[70], K. Pal[70], R. Raturi[70], P. Sadangi[70], S.K. Swain[70], S. Varghese[70,ao], D. Vats[70,ao], A. Alpana[71], S. Dube[71], P. Hazarika[71], B. Kansal[71],

JHEP05(2026)191

A. Laha[71], R. Sharma[71], S. Sharma[71], K.Y. Vaish[71], S. Ghosh[72], H. Bakhshiansohi[73,ap], A. Jafari[73,aq], V. Sedighzadeh Dalavi[73], M. Zeinali[73,ar], S. Bashiri[74], S. Chenarani[74,as], S.M. Etesami[74], Y. Hosseini[74], M. Khakzad[74], E. Khazaie[74], M. Mohammadi Najafabadi[74], S. Tizchang[74,at], M. Felcini[75], M. Grunewald[75], M. Abbrescia[76a,76b], M. Barbieri[76a,76b], M. Buonsante[76a,76b], A. Colaleo[76a,76b], D. Creanza[76a,76c], N. De Filippis[76a,76c], M. De Palma[76a,76b], W. Elmetenawee[76a,76b,au], N. Ferrara[76a,76c], L. Fiore[76a], L. Longo[76a], M. Louka[76a,76b], G. Maggi[76a,76c], M. Maggi[76a], I. Margjeka[76a], V. Mastrapasqua[76a,76b], S. My[76a,76b], F. Nenna[76a,76b], S. Nuzzo[76a,76b], A. Pellecchia[76a,76b], A. Pompili[76a,76b], G. Pugliese[76a,76c], R. Radogna[76a,76b], D. Ramos[76a], A. Ranieri[76a], L. Silvestris[76a], F.M. Simone[76a,76c], A. Stamerra[76a,76b], Ü. Sözbilir[76a], D. Troiano[76a,76b], R. Venditti[76a,76b], P. Verwilligen[76a], A. Zaza[76a,76b], G. Abbiendi[77a], C. Battilana[77a,77b], P. Capiluppi[77a,77b], F.R. Cavallo[77a], M. Cuffiani[77a,77b], G.M. Dallavalle[77a], T. Diotalevi[77a,77b], F. Fabbri[77a], A. Fanfani[77a,77b], R. Farinelli[77a], D. Fasanella[77a], P. Giacomelli[77a], C. Grandi[77a], L. Guiducci[77a,77b], S. Lo Meo[77a,av], M. Lorusso[77a,77b], L. Lunerti[77a], S. Marcellini[77a], G. Masetti[77a], F.L. Navarria[77a,77b], G. Paggi[77a,77b], A. Perrotta[77a], F. Primavera[77a,77b], A.M. Rossi[77a,77b], S. Rossi Tisbeni[77a,77b], T. Rovelli[77a,77b], S. Costa[78a,78b,aw], A. Di Mattia[78a], A. Lapertosa[78a], R. Potenza[78a,78b], A. Tricomi[78a,78b,aw], J. Altork[79a,79b], P. Assiouras[79a], G. Barbagli[79a], G. Bardelli[79a], M. Bartolini[79a,79b], A. Calandri[79a,79b], B. Camaiani[79a,79b], A. Cassese[79a], R. Ceccarelli[79a], V. Ciulli[79a,79b], C. Civinini[79a], R. D'Alessandro[79a,79b], L. Damenti[79a,79b], E. Focardi[79a,79b], T. Kello[79a], G. Latino[79a,79b], P. Lenzi[79a,79b], M. Lizzo[79a], M. Meschini[79a], S. Paoletti[79a], A. Papanastassiou[79a,79b], G. Sguazzoni[79a], L. Viliani[79a], L. Benussi[80], S. Bianco[80], S. Meola[80,ax], D. Piccolo[80], M. Alves Gallo Pereira[81a], F. Ferro[81a], E. Robutti[81a], S. Tosi[81a,81b], A. Benaglia[82a], F. Brivio[82a], V. Camagni[82a,82b], F. Cetorelli[82a,82b], F. De Guio[82a,82b], M.E. Dinardo[82a,82b], P. Dini[82a], S. Gennai[82a], R. Gerosa[82a,82b], A. Ghezzi[82a,82b], P. Govoni[82a,82b], L. Guzzi[82a], M.R. Kim[82a], G. Lavizzari[82a,82b], M.T. Lucchini[82a,82b], M. Malberti[82a], S. Malvezzi[82a], A. Massironi[82a], D. Menasce[82a], L. Moroni[82a], M. Paganoni[82a,82b], S. Palluotto[82a,82b], D. Pedrini[82a], A. Perego[82a,82b], G. Pizzati[82a,82b], S. Ragazzi[82a,82b], T. Tabarelli de Fatis[82a,82b], S. Buontempo[83a], C. Di Fraia[83a,83b], F. Fabozzi[83a,83c], L. Favilla[83a,83d], A.O.M. Iorio[83a,83b], L. Lista[83a,83b,ay], P. Paolucci[83a,ac], B. Rossi[83a], P. Azzi[84a], N. Bacchetta[84a,az], M. Bellato[84a], D. Bisello[84a,84b], P. Bortignon[84a,84c], G. Bortolato[84a,84b], A.C.M. Bulla[84a,84c], R. Carlin[84a,84b], T. Dorigo[84a,ba], F. Gasparini[84a,84b], S. Giorgetti[84a], E. Lusiani[84a], M. Margoni[84a,84b], A.T. Meneguzzo[84a,84b], J. Pazzini[84a,84b], P. Ronchese[84a,84b], R. Rossin[84a,84b], F. Simonetto[84a,84b], M. Tosi[84a,84b], A. Triossi[84a,84b], S. Ventura[84a], M. Zanetti[84a,84b], P. Zotto[84a,84b], A. Zucchetta[84a,84b], G. Zumerle[84a,84b], A. Braghieri[85a], S. Calzaferri[85a], P. Montagna[85a,85b], M. Pelliccioni[85a], V. Re[85a], C. Riccardi[85a,85b], P. Salvini[85a], I. Vai[85a,85b], P. Vitulo[85a,85b], S. Ajmal[86a,86b], M.E. Ascioti[86a,86b], G.M. Bilei[86a], C. Carrivale[86a,86b], D. Ciangottini[86a,86b], L. Della Penna[86a,86b], L. Fanò[86a,86b,†], V. Mariani[86a,86b], M. Menichelli[86a], F. Moscatelli[86a,bb], A. Rossi[86a,86b], A. Santocchia[86a,86b], D. Spiga[86a], T. Tedeschi[86a,86b], C. Aimè[87a,87b], C.A. Alexe[87a,87c], P. Asenov[87a,87b], P. Azzurri[87a], G. Bagliesi[87a], L. Bianchini[87a,87b], T. Boccali[87a], E. Bossini[87a], D. Bruschini[87a,87c], L. Calligaris[87a,87b], R. Castaldi[87a], F. Cattafesta[87a,87c],

JHEP05(2026)191

M.A. Ciocci[87a,87d], M. Cipriani[87a,87b], R. Dell'Orso[87a], S. Donato[87a,87b], R. Forti[87a,87b], A. Giassi[87a], F. Ligabue[87a,87c], A.C. Marini[87a,87b], D. Matos Figueiredo[87a], A. Messineo[87a,87b], S. Mishra[87a], V.K. Muraleedharan Nair Bindhu[87a,87b], S. Nandan[87a], F. Palla[87a], M. Riggirello[87a,87c], A. Rizzi[87a,87b], G. Rolandi[87a,87c], S. Roy Chowdhury[87a,bc], T. Sarkar[87a], A. Scribano[87a], P. Solanki[87a,87b], P. Spagnolo[87a], F. Tenchini[87a,87b], R. Tenchini[87a], G. Tonelli[87a,87b], N. Turini[87a,87d], F. Vaselli[87a,87c], A. Venturi[87a], P.G. Verdini[87a], P. Akrap[88a,88b], C. Basile[88a,88b], S.C. Behera[88a], F. Cavallari[88a], L. Cunqueiro Mendez[88a,88b], F. De Riggi[88a,88b], D. Del Re[88a,88b], E. Di Marco[88a], M. Diemoz[88a], F. Errico[88a], L. Frosina[88a,88b], R. Gargiulo[88a,88b], B. Harikrishnan[88a,88b], F. Lombardi[88a,88b], E. Longo[88a,88b], L. Martikainen[88a,88b], J. Mijuskovic[88a,88b], G. Organtini[88a,88b], N. Palmeri[88a,88b], R. Paramatti[88a,88b], S. Rahatlou[88a,88b], C. Rovelli[88a], F. Santanastasio[88a,88b], L. Soffi[88a], V. Vladimirov[88a,88b], N. Amapane[89a,89b], R. Arcidiacono[89a,89c], S. Argiro[89a,89b], M. Arneodo[89a,89c], N. Bartosik[89a,89c], R. Bellan[89a,89b], A. Bellora[89a,89b], C. Biino[89a], C. Borca[89a,89b], N. Cartiglia[89a], M. Costa[89a,89b], R. Covarelli[89a,89b], N. Demaria[89a], L. Finco[89a], M. Grippo[89a,89b], B. Kiani[89a,89b], L. Lanteri[89a,89b], F. Legger[89a], F. Luongo[89a,89b], C. Mariotti[89a], S. Maselli[89a], A. Mecca[89a,89b], L. Menzio[89a,89b], P. Meridiani[89a], E. Migliore[89a,89b], M. Monteno[89a], M.M. Obertino[89a,89b], G. Ortona[89a], L. Pacher[89a,89b], N. Pastrone[89a], M. Ruspa[89a,89c], F. Siviero[89a,89b], V. Sola[89a,89b], A. Solano[89a,89b], A. Staiano[89a], C. Tarricone[89a,89b], D. Trocino[89a], G. Umoret[89a,89b], E. Vlasov[89a,89b], R. White[89a,89b], J. Babbar[90a,90b], S. Belforte[90a], V. Candelise[90a,90b], M. Casarsa[90a], F. Cossutti[90a], K. De Leo[90a], G. Della Ricca[90a,90b], R. Delli Gatti[90a,90b], S. Dogra[91], J. Hong[91], J. Kim[91], T. Kim[91], D. Lee[91], H. Lee[91], J. Lee[91], S.W. Lee[91], C.S. Moon[91], Y.D. Oh[91], S. Sekmen[91], B. Tae[91], Y.C. Yang[91], M.S. Kim[92], G. Bak[93], P. Gwak[93], H. Kim[93], D.H. Moon[93], J. Seo[93], E. Asilar[94], F. Carnevali[94], J. Choi[94,bd], T.J. Kim[94], Y. Ryou[94], S. Ha[95], S. Han[95], B. Hong[95], J. Kim[95], K. Lee[95], K.S. Lee[95], S. Lee[95], J. Yoo[95], J. Goh[96], J. Shin[96], S. Yang[96], Y. Kang[97], H. S. Kim[97], Y. Kim[97], S. Lee[97], J. Almond[98], J.H. Bhyun[98], J. Choi[98], J. Choi[98], W. Jun[98], H. Kim[98], J. Kim[98], T. Kim[98], Y. Kim[98], Y.W. Kim[98], S. Ko[98], H. Lee[98], J. Lee[98], J. Lee[98], B.H. Oh[98], S.B. Oh[98], J. Shin[98], U.K. Yang[98], I. Yoon[98], W. Jang[99], D.Y. Kang[99], D. Kim[99], S. Kim[99], B. Ko[99], J.S.H. Lee[99], Y. Lee[99], I.C. Park[99], Y. Roh[99], I.J. Watson[99], G. Cho[100], K. Hwang[100], B. Kim[100], S. Kim[100], K. Lee[100], H.D. Yoo[100], Y. Lee[101], I. Yu[101], T. Beyrouthy[102], Y. Gharbia[102], F. Alazemi[103], K. Dreimanis[104], O.M. Eberlins[104], A. Gaile[104], C. Munoz Diaz[104], D. Osite[104], G. Pikurs[104], R. Plese[104], A. Potrebko[104], M. Seidel[104], D. Sidiropoulos Kontos[104], N.R. Strautnieks[105], M. Ambrozas[106], A. Juodagalvis[106], S. Nargelas[106], A. Rinkevicius[106], G. Tamulaitis[106], I. Yusuff[107,be], Z. Zolkapli[107], J.F. Benitez[108], A. Castaneda Hernandez[108], A. Cota Rodriguez[108], L.E. Cuevas Picos[108], H.A. Encinas Acosta[108], L.G. Gallegos Maríñez[108], J.A. Murillo Quijada[108], L. Valencia Palomo[108], G. Ayala[109], H. Castilla-Valdez[109], H. Crotte Ledesma[109], R. Lopez-Fernandez[109], J. Mejia Guisao[109], R. Reyes-Almanza[109], A. Sánchez Hernández[109], C. Oropeza Barrera[110], D.L. Ramirez Guadarrama[110], M. Ramírez García[110], I. Bautista[111], F.E. Neri Huerta[111], I. Pedraza[111], H.A. Salazar Ibarguen[111], C. Uribe Estrada[111], I. Bubanja[112], N. Raicevic[112], P.H. Butler[113], A. Ahmad[114], M.I. Asghar[114],

JHEP05(2026)191

A. Awais[114], M.I.M. Awan[114], W.A. Khan[114], V. Avati[115], L. Forthomme[115], L. Grzanka[115], M. Malawski[115], K. Piotrzkowski[115], M. Bluj[116], M. Górski[116], M. Kazana[116], M. Szleper[116], P. Zalewski[116], K. Bunkowski[117], K. Doroba[117], A. Kalinowski[117], M. Konecki[117], J. Krolikowski[117], A. Muhammad[117], P. Fokow[118], K. Pozniak[118], W. Zabolotny[118], M. Araujo[119], D. Bastos[119], C. Beirão Da Cruz E Silva[119], A. Boletti[119], M. Bozzo[119], T. Camporesi[119], G. Da Molin[119], M. Gallinaro[119], J. Hollar[119], N. Leonardo[119], G.B. Marozzo[119], A. Petrilli[119], M. Pisano[119], J. Seixas[119], J. Varela[119], J.W. Wulff[119], P. Adzic[120], L. Markovic[120], P. Milenovic[120], V. Milosevic[120], D. Devetak[121], M. Dordevic[121], J. Milosevic[121], L. Nadderd[121], V. Rekovic[121], M. Stojanovic[121], M. Alcalde Martinez[122], J. Alcaraz Maestre[122], J.A. Brochero Cifuentes[122], M. Cepeda[122], M. Cerrada[122], N. Colino[122], B. De La Cruz[122], A. Delgado Peris[122], A. Escalante Del Valle[122], Cristina F. Bedoya[122], D. Fernández Del Val[122], J.P. Fernández Ramos[122], J. Flix[122], M.C. Fouz[122], M. Gonzalez Hernandez[122], O. Gonzalez Lopez[122], S. Goy Lopez[122], J.M. Hernandez[122], M.I. Josa[122], J. Llorente Merino[122], Oliver M. Carretero[122], C. Martin Perez[122], E. Martin Viscasillas[122], D. Moran[122], C. M. Morcillo Perez[122], Á. Navarro Tobar[122], R. Paz Herrera[122], C. Perez Dengra[122], J. Puerta Pelayo[122], A. Pérez-Calero Yzquierdo[122], I. Redondo[122], J. Vazquez Escobar[122], J.F. de Trocóniz[123], B. Alvarez Gonzalez[124], J. Ayllon Torresano[124], A. Cardini[124], J. Cuevas[124], J. Del Riego Badas[124], D. Estrada Acevedo[124], J. Fernandez Menendez[124], S. Folgueras[124], I. Gonzalez Caballero[124], P. Leguina[124], M. Obeso Menendez[124], E. Palencia Cortezon[124], J. Prado Pico[124], A. Soto Rodríguez[124], C. Vico Villalba[124], P. Vischia[124], S. Blanco Fernández[125], I.J. Cabrillo[125], A. Calderon[125], J. Duarte Campderros[125], M. Fernandez[125], G. Gomez[125], C. Lasaosa García[125], R. Lopez Ruiz[125], C. Martinez Rivero[125], P. Martinez Ruiz del Arbol[125], F. Matorras[125], P. Matorras Cuevas[125], E. Navarrete Ramos[125], J. Piedra Gomez[125], C. Quintana San Emeterio[125], L. Scodellaro[125], I. Vila[125], R. Vilar Cortabitarte[125], J.M. Vizan Garcia[125], D.D.C. Wickramarathna[126], B. Kailasapathy[126,bf], W.G.D. Dharmaratna[127,bg], K. Liyanage[127], N. Perera[127], D. Abbaneo[128], C. Amendola[128], R. Ardino[128], E. Auffray[128], J. Baechler[128], D. Barney[128], J. Bendavid[128], M. Bianco[128], A. Bocci[128], L. Borgonovi[128], C. Botta[128], A. Bragagnolo[128], C.E. Brown[128], C. Caillol[128], G. Cerminara[128], P. Connor[128], D. d'Enterria[128], A. Dabrowski[128], A. David[128], A. De Roeck[128], M.M. Defranchis[128], M. Deile[128], M. Dobson[128], P.J. Fernández Manteca[128], B.A. Fontana Santos Alves[128], W. Funk[128], A. Gaddi[128], S. Giani[128], D. Gigi[128], K. Gill[128], F. Glege[128], M. Glowacki[128], A. Gruber[128], J. Hegeman[128], J.K. Heikkilä[128], R. Hofsaess[128], B. Huber[128], T. James[128], P. Janot[128], O. Kaluzinska[128], O. Karacheban[128,z], G. Karathanasis[128], S. Laurila[128], P. Lecoq[128], E. Leutgeb[128], C. Lourenço[128], A.-M. Lyon[128], M. Magherini[128], L. Malgeri[128], M. Mannelli[128], A. Mehta[128], F. Meijers[128], J.A. Merlin[128], S. Mersi[128], E. Meschi[128], M. Migliorini[128], F. Monti[128], F. Moortgat[128], M. Mulders[128], M. Musich[128], I. Neutelings[128], S. Orfanelli[128], F. Pantaleo[128], M. Pari[128], G. Petrucciani[128], A. Pfeiffer[128], M. Pierini[128], M. Pitt[128], H. Qu[128], D. Rabady[128], A. Reimers[128], B. Ribeiro Lopes[128], F. Riti[128], P. Rosado[128], M. Rovere[128], H. Sakulin[128], R. Salvatico[128], S. Sanchez Cruz[128], S. Scarfi[128], M. Selvaggi[128], A. Sharma[128],

JHEP05(2026)191

K. Shchelina[128], P. Silva[128], P. Sphicas[128,bh], A.G. Stahl Leiton[128], A. Steen[128], S. Summers[128], D. Treille[128], P. Tropea[128], E. Vernazza[128], J. Wanczyk[128,bi], J. Wang[128], S. Wuchterl[128], M. Zarucki[128], P. Zehetner[128], P. Zejdl[128], G. Zevi Della Porta[128], T. Bevilacqua[129,bj], L. Caminada[129,bj], W. Erdmann[129], R. Horisberger[129], Q. Ingram[129], H.C. Kaestli[129], D. Kotlinski[129], C. Lange[129], U. Langenegger[129], L. Noehte[129,bj], T. Rohe[129], A. Samalan[129], T.K. Aarrestad[130], M. Backhaus[130], G. Bonomelli[130], C. Cazzaniga[130], K. Datta[130], P. De Bryas Dexmiers D'Archiacchiac[130,bi], A. De Cosa[130], G. Dissertori[130], M. Dittmar[130], M. Donegà[130], F. Eble[130], K. Gedia[130], F. Glessgen[130], C. Grab[130], T.G. Harte[130], N. Härringer[130], W. Lustermann[130], M. Malucchi[130], R.A. Manzoni[130], L. Marchese[130], A. Mascellani[130,bi], F. Nessi-Tedaldi[130], F. Pauss[130], V. Perovic[130], B. Ristic[130], R. Seidita[130], J. Steggemann[130,bi], A. Tarabini[130], D. Valsecchi[130], R. Wallny[130], C. Amsler[131,bk], F. Bilandzija[131], P. Bärtschi[131], M.F. Canelli[131], G. Celotto[131], K. Cormier[131], M. Huwiler[131], W. Jin[131], A. Jofrehei[131], B. Kilminster[131], T.H. Kwok[131], S. Leontsinis[131], V. Lukashenko[131], A. Macchiolo[131], F. Meng[131], M. Missiroli[131], J. Motta[131], P. Robmann[131], M. Senger[131], E. Shokr[131], F. Stäger[131], R. Tramontano[131], P. Viscone[131], D. Bhowmik[132], C.M. Kuo[132], P.K. Rout[132], S. Taj[132], P.C. Tiwari[132,al], L. Ceard[133], K.F. Chen[133], Z.g. Chen[133], A. De Iorio[133], W.-S. Hou[133], T.h. Hsu[133], Y.w. Kao[133], S. Karmakar[133], G. Kole[133], Y.y. Li[133], R.-S. Lu[133], E. Paganis[133], X.f. Su[133], J. Thomas-Wilsker[133], L.s. Tsai[133], D. Tsionou[133], H.y. Wu[133], E. Yazgan[133], C. Asawatangtrakuldee[134], N. Srimanobhas[134], Y. Maghrbi[135], D. Agyel[136], F. Dolek[136], I. Dumanoglu[136,bl], Y. Guler[136,bm], E. Gurpinar Guler[136,bm], C. Isik[136], O. Kara[136], A. Kayis Topaksu[136], Y. Komurcu[136], G. Onengut[136], K. Ozdemir[136,bn], B. Tali[136,bo], U.G. Tok[136], E. Uslan[136], I.S. Zorbakir[136], S. Sen[137], M. Yalvac[138,bp], B. Akgun[139], I.O. Atakisi[139,bq], E. Gülmez[139], M. Kaya[139,br], O. Kaya[139,bs], M.A. Sarkisla[139,bt], S. Tekten[139,bu], D. Boncukcu[140], A. Cakir[140], K. Cankocak[140,bl,bv], B. Hacisahinoglu[141], I. Hos[141,bw], B. Kaynak[141], S. Ozkorucuklu[141], O. Potok[141], H. Sert[141], C. Simsek[141], C. Zorbilmez[141], S. Cerci[142], C. Dozen[142,bx], B. Isildak[142,by], E. Simsek[142], D. Sunar Cerci[142], T. Yetkin[142,bx], A. Boyaryntsev[143], O. Dadazhanova[143], B. Grynyov[143], L. Levchuk[144], J.J. Brooke[145], A. Bundock[145], F. Bury[145], E. Clement[145], D. Cussans[145], D. Dharmender[145], H. Flacher[145], J. Goldstein[145], H.F. Heath[145], M.-L. Holmberg[145], L. Kreczko[145], S. Paramesvaran[145], L. Robertshaw[145], M.S. Sanjrani[145,ap], J. Segal[145], V.J. Smith[145], A.H. Ball[146], K.W. Bell[146], A. Belyaev[146,bz], C. Brew[146], R.M. Brown[146], D.J.A. Cockerill[146], A. Elliot[146], K.V. Ellis[146], J. Gajownik[146], K. Harder[146], S. Harper[146], J. Linacre[146], K. Manolopoulos[146], M. Moallemi[146], D.M. Newbold[146], E. Olaiya[146], D. Petyt[146], T. Reis[146], A.R. Sahasransu[146], G. Salvi[146], T. Schuh[146], C.H. Shepherd-Themistocleous[146], I.R. Tomalin[146], K.C. Whalen[146], T. Williams[146], I. Andreou[147], R. Bainbridge[147], P. Bloch[147], O. Buchmuller[147], C.A. Carrillo Montoya[147], D. Colling[147], I. Das[147], P. Dauncey[147], G. Davies[147], M. Della Negra[147], S. Fayer[147], G. Fedi[147], G. Hall[147], H.R. Hoorani[147], A. Howard[147], G. Iles[147], C.R. Knight[147], P. Krueper[147], J. Langford[147], K.H. Law[147], J. León Holgado[147], L. Lyons[147], A.-M. Magnan[147], B. Maier[147], S. Mallios[147], A. Mastronikolis[147], M. Mieskolainen[147], J. Nash[147,ca], M. Pesaresi[147], P.B. Pradeep[147], B.C. Radburn-Smith[147], A. Richards[147], A. Rose[147], L. Russell[147],

JHEP05(2026)191

K. Savva[147], C. Seez[147], R. Shukla[147], A. Tapper[147], K. Uchida[147], G.P. Uttley[147], T. Virdee[147,ac], M. Vojinovic[147], N. Wardle[147], D. Winterbottom[147], J.E. Cole[148], A. Khan[148], P. Kyberd[148], I.D. Reid[148], S. Abdullin[149], A. Brinkerhoff[149], E. Collins[149], M.R. Darwish[149], J. Dittmann[149], K. Hatakeyama[149], V. Hegde[149], J. Hiltbrand[149], B. McMaster[149], J. Samudio[149], S. Sawant[149], C. Sutantawibul[149], J. Wilson[149], J.M. Hogan[150], R. Bartek[151], A. Dominguez[151], S. Raj[151], A.E. Simsek[151], S.S. Yu[151], B. Bam[152], A. Buchot Perraguin[152], S. Campbell[152], R. Chudasama[152], S.I. Cooper[152], C. Crovella[152], G. Fidalgo[152], S.V. Gleyzer[152], A. Khukhunaishvili[152], K. Matchev[152], E. Pearson[152], C.U. Perez[152], P. Rumerio[152,cb], E. Usai[152], R. Yi[152], S. Cholak[153], G. De Castro[153], Z. Demiragli[153], C. Erice[153], C. Fangmeier[153], C. Fernandez Madrazo[153], E. Fontanesi[153], J. Fulcher[153], F. Golf[153], S. Jeon[153], J. O'Cain[153], I. Reed[153], J. Rohlf[153], K. Salyer[153], D. Sperka[153], D. Spitzbart[153], I. Suarez[153], A. Tsatsos[153], E. Wurtz[153], A.G. Zecchinelli[153], G. Barone[154], G. Benelli[154], D. Cutts[154], S. Ellis[154], L. Gouskos[154], M. Hadley[154], U. Heintz[154], K.W. Ho[154], T. Kwon[154], L. Lambrecht[154], G. Landsberg[154], K.T. Lau[154], J. Luo[154], S. Mondal[154], J. Roloff[154], T. Russell[154], S. Sagir[154,cc], X. Shen[154], M. Stamenkovic[154], N. Venkatasubramanian[154], S. Abbott[155], S. Baradia[155], B. Barton[155], R. Breedon[155], H. Cai[155], M. Calderon De La Barca Sanchez[155], E. Cannaert[155], M. Chertok[155], M. Citron[155], J. Conway[155], P.T. Cox[155], R. Erbacher[155], O. Kukral[155], G. Mocellin[155], S. Ostrom[155], I. Salazar Segovia[155], J.S. Tafoya Vargas[155], W. Wei[155], S. Yoo[155], K. Adamidis[156], M. Bachtis[156], D. Campos[156], R. Cousins[156], A. Datta[156], G. Flores Avila[156], J. Hauser[156], M. Ignatenko[156], M.A. Iqbal[156], T. Lam[156], Y.f. Lo[156], E. Manca[156], A. Nunez Del Prado[156], D. Saltzberg[156], V. Valuev[156], R. Clare[157], J.W. Gary[157], G. Hanson[157], A. Aportela[158], A. Arora[158], J.G. Branson[158], S. Cittolin[158], S. Cooperstein[158], B. D'Anzi[158], D. Diaz[158], J. Duarte[158], L. Giannini[158], Y. Gu[158], J. Guiang[158], V. Krutelyov[158], R. Lee[158], J. Letts[158], H. Li[158], M. Masciovecchio[158], F. Mokhtar[158], S. Mukherjee[158], M. Pieri[158], D. Primosch[158], M. Quinnan[158], V. Sharma[158], M. Tadel[158], E. Vourliotis[158], F. Würthwein[158], A. Yagil[158], Z. Zhao[158], A. Barzdukas[159], L. Brennan[159], C. Campagnari[159], S. Carron Montero[159,cd], K. Downham[159], C. Grieco[159], M.M. Hussain[159], J. Incandela[159], M.W.K. Lai[159], A.J. Li[159], P. Masterson[159], J. Richman[159], S.N. Santpur[159], U. Sarica[159], R. Schmitz[159], F. Setti[159], J. Sheplock[159], D. Stuart[159], T.Á. Vámi[159], X. Yan[159], D. Zhang[159], A. Albert[160], S. Bhattacharya[160], A. Bornheim[160], O. Cerri[160], R. Kansal[160], J. Mao[160], H.B. Newman[160], G. Reales Gutiérrez[160], T. Sievert[160], M. Spiropulu[160], J.R. Vlimant[160], R.A. Wynne[160], S. Xie[160], J. Alison[161], S. An[161], M. Cremonesi[161], V. Dutta[161], E.Y. Ertorer[161], T. Ferguson[161], T.A. Gómez Espinosa[161], A. Harilal[161], A. Kallil Tharayil[161], M. Kanemura[161], C. Liu[161], M. Marchegiani[161], P. Meiring[161], T. Mudholkar[161], S. Murthy[161], P. Palit[161], K. Park[161], M. Paulini[161], A. Roberts[161], A. Sanchez[161], W. Terrill[161], J.P. Cumalat[162], W.T. Ford[162], A. Hart[162], S. Kwan[162], J. Pearkes[162], C. Savard[162], N. Schonbeck[162], K. Stenson[162], K.A. Ulmer[162], S.R. Wagner[162], N. Zipper[162], D. Zuolo[162], J. Alexander[163], X. Chen[163], J. Dickinson[163], A. Duquette[163], J. Fan[163], X. Fan[163], J. Grassi[163], S. Hogan[163], P. Kotamnives[163], J. Monroy[163], G. Niendorf[163], M. Oshiro[163], J.R. Patterson[163], A. Ryd[163], J. Thom[163],

JHEP05(2026)191

P. Wittich[163], R. Zou[163], L. Zygala[163], M. Albrow[164], M. Alyari[164], O. Amram[164], G. Apollinari[164], A. Apresyan[164], L.A.T. Bauerdick[164], D. Berry[164], J. Berryhill[164], P.C. Bhat[164], K. Burkett[164], J.N. Butler[164], A. Canepa[164], G.B. Cerati[164], H.W.K. Cheung[164], F. Chlebana[164], C. Cosby[164], G. Cummings[164], I. Dutta[164], V.D. Elvira[164], J. Freeman[164], A. Gandrakota[164], Z. Gecse[164], L. Gray[164], D. Green[164], A. Grummer[164], S. Grünendahl[164], D. Guerrero[164], O. Gutsche[164], R.M. Harris[164], T.C. Herwig[164], J. Hirschauer[164], V. Innocente[164], B. Jayatilaka[164], S. Jindariani[164], M. Johnson[164], U. Joshi[164], B. Klima[164], K.H.M. Kwok[164], S. Lammel[164], C. Lee[164], D. Lincoln[164], R. Lipton[164], T. Liu[164], K. Maeshima[164], D. Mason[164], P. McBride[164], P. Merkel[164], S. Mrenna[164], S. Nahn[164], J. Ngadiuba[164], D. Noonan[164], S. Norberg[164], V. Papadimitriou[164], N. Pastika[164], K. Pedro[164], C. Pena[164,ce], C.E. Perez Lara[164], F. Ravera[164], A. Reinsvold Hall[164,cf], L. Ristori[164], M. Safdari[164], E. Sexton-Kennedy[164], N. Smith[164], A. Soha[164], L. Spiegel[164], S. Stoynev[164], J. Strait[164], L. Taylor[164], S. Tkaczyk[164], N.V. Tran[164], L. Uplegger[164], E.W. Vaandering[164], C. Wang[164], I. Zoi[164], C. Aruta[165], P. Avery[165], D. Bourilkov[165], P. Chang[165], V. Cherepanov[165], R.D. Field[165], C. Huh[165], E. Koenig[165], M. Kolosova[165], J. Konigsberg[165], A. Korytov[165], G. Mitselmakher[165], K. Mohrman[165], A. Muthirakalayil Madhu[165], N. Rawal[165], S. Rosenzweig[165], V. Sulimov[165], Y. Takahashi[165], J. Wang[165], T. Adams[166], A. Al Kadhim[166], A. Askew[166], S. Bower[166], R. Goff[166], R. Hashmi[166], A. Hassani[166], R.S. Kim[166], T. Kolberg[166], G. Martinez[166], M. Mazza[166], H. Prosper[166], P.R. Prova[166], R. Yohay[166], B. Alsufyani[167], S. Butalla[167], S. Das[167], M. Hohlmann[167], M. Lavinsky[167], E. Yanes[167], M.R. Adams[168], N. Barnett[168], A. Baty[168], C. Bennett[168], R. Cavanaugh[168], R. Escobar Franco[168], O. Evdokimov[168], C.E. Gerber[168], H. Gupta[168], M. Hawksworth[168], A. Hingrajiya[168], D.J. Hofman[168], J.h. Lee[168], C. Mills[168], S. Nanda[168], G. Nigmatkulov[168], B. Ozek[168], T. Phan[168], D. Pilipovic[168], R. Pradhan[168], E. Prifti[168], P. Roy[168], T. Roy[168], N. Singh[168], M.B. Tonjes[168], N. Varelas[168], M.A. Wadud[168], J. Yoo[168], M. Alhusseini[169], D. Blend[169], K. Dilsiz[169,cg], O.K. Köseyan[169], A. Mestvirishvili[169,ch], O. Neogi[169], H. Ogul[169,ci], Y. Onel[169], A. Penzo[169], C. Snyder[169], E. Tiras[169,cj], B. Blumenfeld[170], J. Davis[170], A.V. Gritsan[170], L. Kang[170], S. Kyriacou[170], P. Maksimovic[170], M. Roguljic[170], S. Sekhar[170], M.V. Srivastav[170], M. Swartz[170], A. Abreu[171], L.F. Alcerro Alcerro[171], J. Anguiano[171], S. Arteaga Escatel[171], P. Baringer[171], A. Bean[171], R. Bhattacharya[171], Z. Flowers[171], D. Grove[171], J. King[171], G. Krintiras[171], M. Lazarovits[171], C. Le Mahieu[171], J. Marquez[171], M. Murray[171], M. Nickel[171], S. Popescu[171,ck], C. Rogan[171], C. Royon[171], S. Rudrabhatla[171], S. Sanders[171], C. Smith[171], G. Wilson[171], B. Allmond[172], N. Islam[172], A. Ivanov[172], K. Kaadze[172], Y. Maravin[172], J. Natoli[172], G.G. Reddy[172], D. Roy[172], G. Sorrentino[172], A. Baden[173], A. Belloni[173], J. Bistany-riebman[173], S.C. Eno[173], N.J. Hadley[173], S. Jabeen[173], R.G. Kellogg[173], T. Koeth[173], B. Kronheim[173], S. Lascio[173], P. Major[173], A.C. Mignerey[173], C. Palmer[173], C. Papageorgakis[173], M.M. Paranjpe[173], E. Popova[173,cl], A. Shevelev[173], L. Zhang[173], C. Baldenegro Barrera[174], H. Bossi[174], S. Bright-Thonney[174], I.A. Cali[174], Y.c. Chen[174], P.c. Chou[174], M. D'Alfonso[174], J. Eysermans[174], C. Freer[174], G. Gomez-Ceballos[174], M. Goncharov[174], G. Grosso[174], P. Harris[174], D. Hoang[174], G.M. Innocenti[174], K. Ivanov[174], D. Kovalskyi[174], J. Krupa[174], L. Lavezzo[174],

JHEP05(2026)191

Y.-J. Lee[174], K. Long[174], C. Mcginn[174], A. Novak[174], M.I. Park[174], C. Paus[174], C. Reissel[174], C. Roland[174], G. Roland[174], S. Rothman[174], T.a. Sheng[174], G.S.F. Stephans[174], D. Walter[174], Z. Wang[174], B. Wyslouch[174], T. J. Yang[174], B. Crossman[175], W.J. Jackson[175], C. Kapsiak[175], M. Krohn[175], D. Mahon[175], J. Mans[175], B. Marzocchi[175], R. Rusack[175], O. Sancar[175], R. Saradhy[175], N. Strobbe[175], K. Bloom[176], D.R. Claes[176], G. Haza[176], J. Hossain[176], C. Joo[176], I. Kravchenko[176], A. Rohilla[176], J.E. Siado[176], W. Tabb[176], A. Vagnerini[176], A. Wightman[176], F. Yan[176], H. Bandyopadhyay[177], L. Hay[177], H.w. Hsia[177], I. Iashvili[177], A. Kalogeropoulos[177], A. Kharchilava[177], A. Mandal[177], M. Morris[177], D. Nguyen[177], S. Rappoccio[177], H. Rejeb Sfar[177], A. Williams[177], P. Young[177], D. Yu[177], G. Alverson[178], E. Barberis[178], J. Bonilla[178], B. Bylsma[178], M. Campana[178], J. Dervan[178], Y. Haddad[178], Y. Han[178], I. Israr[178], A. Krishna[178], M. Lu[178], N. Manganelli[178], R. Mccarthy[178], D.M. Morse[178], T. Orimoto[178], L. Skinnari[178], C.S. Thoreson[178], E. Tsai[178], D. Wood[178], S. Dittmer[179], K.A. Hahn[179], M. Mcginnis[179], Y. Miao[179], D.G. Monk[179], M.H. Schmitt[179], A. Taliercio[179], M. Velasco[179], J. Wang[179], G. Agarwal[180], R. Band[180], R. Bucci[180], S. Castells[180], A. Das[180], A. Ehnis[180], R. Goldouzian[180], M. Hildreth[180], K. Hurtado Anampa[180], T. Ivanov[180], C. Jessop[180], A. Karneyeu[180], K. Lannon[180], J. Lawrence[180], N. Loukas[180], L. Lutton[180], J. Mariano[180], N. Marinelli[180], I. Mcalister[180], T. McCauley[180], C. Mcgrady[180], C. Moore[180], Y. Musienko[180,cm], H. Nelson[180], M. Osherson[180], A. Piccinelli[180], R. Ruchti[180], A. Townsend[180], Y. Wan[180], M. Wayne[180], H. Yockey[180], A. Basnet[181], M. Carrigan[181], R. De Los Santos[181], L.S. Durkin[181], C. Hill[181], M. Joyce[181], M. Nunez Ornelas[181], D.A. Wenzl[181], B.L. Winer[181], B. R. Yates[181], H. Bouchamaoui[182], G. Dezoort[182], P. Elmer[182], A. Frankenthal[182], M. Galli[182], B. Greenberg[182], N. Haubrich[182], K. Kennedy[182], G. Kopp[182], Y. Lai[182], D. Lange[182], A. Loeliger[182], D. Marlow[182], I. Ojalvo[182], J. Olsen[182], F. Simpson[182], D. Stickland[182], C. Tully[182], S. Malik[183], R. Sharma[183], S. Chandra[184], R. Chawla[184], A. Gu[184], L. Gutay[184], M. Jones[184], A.W. Jung[184], D. Kondratyev[184], M. Liu[184], G. Negro[184], N. Neumeister[184], G. Paspalaki[184], S. Piperov[184], N.R. Saha[184], J.F. Schulte[184], F. Wang[184], A. Wildridge[184], W. Xie[184], Y. Yao[184], Y. Zhong[184], N. Parashar[185], A. Pathak[185], E. Shumka[185], D. Acosta[186], A. Agrawal[186], C. Arbour[186], T. Carnahan[186], P. Das[186], K.M. Ecklund[186], S. Freed[186], F.J.M. Geurts[186], T. Huang[186], I. Krommydas[186], N. Lewis[186], W. Li[186], J. Lin[186], O. Miguel Colin[186], B.P. Padley[186], R. Redjimi[186], J. Rotter[186], M. Wulansatiti[186], E. Yigitbasi[186], Y. Zhang[186], O. Bessidskaia Bylund[187], A. Bodek[187], P. de Barbaro[187,†], R. Demina[187], A. Garcia-Bellido[187], H.S. Hare[187], O. Hindrichs[187], N. Parmar[187], P. Parygin[187,cl], H. Seo[187], R. Taus[187], B. Chiarito[188], J.P. Chou[188], S.V. Clark[188], S. Donnelly[188], D. Gadkari[188], Y. Gershtein[188], E. Halkiadakis[188], C. Houghton[188], D. Jaroslawski[188], A. Kobert[188], S. Konstantinou[188], I. Laflotte[188], A. Lath[188], J. Martins[188], M. Perez Prada[188], B. Rand[188], J. Reichert[188], P. Saha[188], S. Salur[188], S. Schnetzer[188], S. Somalwar[188], R. Stone[188], S.A. Thayil[188], S. Thomas[188], J. Vora[188], D. Ally[189], A.G. Delannoy[189], S. Fiorendi[189], J. Harris[189], T. Holmes[189], A.R. Kanuganti[189], N. Karunarathna[189], J. Lawless[189], L. Lee[189], E. Nibigira[189], B. Skipworth[189], S. Spanier[189], D. Aebi[190], M. Ahmad[190], T. Akhter[190], K. Androsov[190], A. Bolshov[190], O. Bouhali[190,cn],

JHEP05(2026)191

A. Cagnotta[190], V. D'Amante[190], R. Eusebi[190], P. Flanagan[190], J. Gilmore[190], Y. Guo[190], T. Kamon[190], S. Luo[190], R. Mueller[190], A. Safonov[190], N. Akchurin[191], J. Damgov[191], Y. Feng[191], N. Gogate[191], Y. Kazhykarim[191], K. Lamichhane[191], S.W. Lee[191], C. Madrid[191], A. Mankel[191], T. Peltola[191], I. Volobouev[191], E. Appelt[192], Y. Chen[192], S. Greene[192], A. Gurrola[192], W. Johns[192], R. Kunnawalkam Elayavalli[192], A. Melo[192], D. Rathjens[192], F. Romeo[192], P. Sheldon[192], S. Tuo[192], J. Velkovska[192], J. Viinikainen[192], J. Zhang[192], B. Cardwell[193], H. Chung[193], B. Cox[193], J. Hakala[193], G. Hamilton Ilha Machado[193], R. Hirosky[193], M. Jose[193], A. Ledovskoy[193], C. Mantilla[193], C. Neu[193], C. Ramón Álvarez[193], Z. Wu[193], S. Bhattacharya[194], P.E. Karchin[194], A. Aravind[195], S. Banerjee[195], K. Black[195], T. Bose[195], E. Chavez[195], S. Dasu[195], P. Everaerts[195], C. Galloni[195], H. He[195], M. Herndon[195], A. Herve[195], C.K. Koraka[195], S. Lomte[195], R. Loveless[195], A. Mallampalli[195], A. Mohammadi[195], S. Mondal[195], T. Nelson[195], G. Parida[195], D. Pinna[195], L. Pétré[195], A. Savin[195], V. Shang[195], V. Sharma[195], W.H. Smith[195], D. Teague[195], H.F. Tsoi[195], W. Vetens[195], A. Warden[195], S. Afanasiev[196], V. Alexakhin[196], Yu. Andreev[196], T. Aushev[196], D. Budkouski[196], R. Chistov[196], M. Danilov[196], T. Dimova[196], A. Ershov[196], S. Gninenko[196], I. Gorbunov[196], A. Gribushin[196], A. Kamenev[196], V. Karjavine[196], M. Kirsanov[196], V. Klyukhin[196], O. Kodolova[196,co], V. Korenkov[196], I. Korsakov[196], A. Kozyrev[196], N. Krasnikov[196], A. Lanev[196], A. Malakhov[196], V. Matveev[196], A. Nikitenko[196,cp,cq], V. Palichik[196], V. Perelygin[196], S. Petrushanko[196], S. Polikarpov[196], O. Radchenko[196], M. Savina[196], V. Shalaev[196], S. Shmatov[196], S. Shulha[196], Y. Skovpen[196], K. Slizhevskiy[196], V. Smirnov[196], O. Teryaev[196], I. Tlisova[196], A. Toropin[196], N. Voytishin[196], A. Zarubin[196], I. Zhizhin[196], E. Boos[197], V. Bunichev[197], M. Dubinin[197,ce], L. Dudko[197], V. Kim[197,cm], V. Murzin[197], V. Oreshkin[197], V. Savrin[197], A. Snigirev[197], D. Sosnov[197]

[1] *Yerevan Physics Institute, Yerevan, Armenia*
[2] *Institut für Hochenergiephysik, Vienna, Austria*
[3] *Universiteit Antwerpen, Antwerpen, Belgium*
[4] *Vrije Universiteit Brussel, Brussel, Belgium*
[5] *Université Libre de Bruxelles, Bruxelles, Belgium*
[6] *Ghent University, Ghent, Belgium*
[7] *Université Catholique de Louvain, Louvain-la-Neuve, Belgium*
[8] *Centro Brasileiro de Pesquisas Fisicas, Rio de Janeiro, Brazil*
[9] *Universidade do Estado do Rio de Janeiro, Rio de Janeiro, Brazil*
[10] *Universidade Estadual Paulista, Universidade Federal do ABC, São Paulo, Brazil*
[11] *Institute for Nuclear Research and Nuclear Energy, Bulgarian Academy of Sciences, Sofia, Bulgaria*
[12] *University of Sofia, Sofia, Bulgaria*
[13] *Instituto De Alta Investigación, Universidad de Tarapacá, Casilla 7 D, Arica, Chile*
[14] *Universidad Tecnica Federico Santa Maria, Valparaiso, Chile*
[15] *Beihang University, Beijing, China*
[16] *Department of Physics, Tsinghua University, Beijing, China*
[17] *Institute of High Energy Physics, Beijing, China*
[18] *State Key Laboratory of Nuclear Physics and Technology, Peking University, Beijing, China*
[19] *State Key Laboratory of Nuclear Physics and Technology, Institute of Quantum Matter, South China Normal University, Guangzhou, China*
[20] *Sun Yat-Sen University, Guangzhou, China*
[21] *University of Science and Technology of China, Hefei, China*

JHEP05(2026)191

[22] Nanjing Normal University, Nanjing, China
[23] Institute of Modern Physics and Key Laboratory of Nuclear Physics and Ion-beam Application (MOE) – Fudan University, Shanghai, China
[24] Zhejiang University, Hangzhou, Zhejiang, China
[25] Universidad de Los Andes, Bogota, Colombia
[26] Universidad de Antioquia, Medellin, Colombia
[27] University of Split, Faculty of Electrical Engineering, Mechanical Engineering and Naval Architecture, Split, Croatia
[28] University of Split, Faculty of Science, Split, Croatia
[29] Institute Rudjer Boskovic, Zagreb, Croatia
[30] University of Cyprus, Nicosia, Cyprus
[31] Charles University, Prague, Czech Republic
[32] Escuela Politecnica Nacional, Quito, Ecuador
[33] Universidad San Francisco de Quito, Quito, Ecuador
[34] Academy of Scientific Research and Technology of the Arab Republic of Egypt, Egyptian Network of High Energy Physics, Cairo, Egypt
[35] Center for High Energy Physics (CHEP-FU), Fayoum University, El-Fayoum, Egypt
[36] National Institute of Chemical Physics and Biophysics, Tallinn, Estonia
[37] Department of Physics, University of Helsinki, Helsinki, Finland
[38] Helsinki Institute of Physics, Helsinki, Finland
[39] Lappeenranta-Lahti University of Technology, Lappeenranta, Finland
[40] IRFU, CEA, Université Paris-Saclay, Gif-sur-Yvette, France
[41] Laboratoire Leprince-Ringuet, CNRS/IN2P3, Ecole Polytechnique, Institut Polytechnique de Paris, Palaiseau, France
[42] Université de Strasbourg, CNRS, IPHC UMR 7178, Strasbourg, France
[43] Centre de Calcul de l'Institut National de Physique Nucleaire et de Physique des Particules, CNRS/IN2P3, Villeurbanne, France
[44] Institut de Physique des 2 Infinis de Lyon (IP2I), Villeurbanne, France
[45] Georgian Technical University, Tbilisi, Georgia
[46] RWTH Aachen University, I. Physikalisches Institut, Aachen, Germany
[47] RWTH Aachen University, III. Physikalisches Institut A, Aachen, Germany
[48] RWTH Aachen University, III. Physikalisches Institut B, Aachen, Germany
[49] Deutsches Elektronen-Synchrotron, Hamburg, Germany
[50] University of Hamburg, Hamburg, Germany
[51] Karlsruher Institut fuer Technologie, Karlsruhe, Germany
[52] Institute of Nuclear and Particle Physics (INPP), NCSR Demokritos, Aghia Paraskevi, Greece
[53] National and Kapodistrian University of Athens, Athens, Greece
[54] National Technical University of Athens, Athens, Greece
[55] University of Ioánnina, Ioánnina, Greece
[56] HUN-REN Wigner Research Centre for Physics, Budapest, Hungary
[57] MTA-ELTE Lendület CMS Particle and Nuclear Physics Group, Eötvös Loránd University, Budapest, Hungary
[58] Faculty of Informatics, University of Debrecen, Debrecen, Hungary
[59] HUN-REN ATOMKI – Institute of Nuclear Research, Debrecen, Hungary
[60] Karoly Robert Campus, MATE Institute of Technology, Gyongyos, Hungary
[61] Panjab University, Chandigarh, India
[62] University of Delhi, Delhi, India
[63] University of Hyderabad, Hyderabad, India
[64] Indian Institute of Technology Kanpur, Kanpur, India
[65] Saha Institute of Nuclear Physics, HBNI, Kolkata, India
[66] Indian Institute of Technology Madras, Madras, India
[67] IISER Mohali, India, Mohali, India
[68] Tata Institute of Fundamental Research-A, Mumbai, India

JHEP05(2026)191

[69] *Tata Institute of Fundamental Research-B, Mumbai, India*
[70] *National Institute of Science Education and Research, An OCC of Homi Bhabha National Institute, Bhubaneswar, Odisha, India*
[71] *Indian Institute of Science Education and Research (IISER), Pune, India*
[72] *Indian Institute of Technology Hyderabad, Telangana, India*
[73] *Isfahan University of Technology, Isfahan, Iran*
[74] *Institute for Research in Fundamental Sciences (IPM), Tehran, Iran*
[75] *University College Dublin, Dublin, Ireland*
[76a] *INFN Sezione di Bari, Bari, Italy*
[76b] *Università di Bari, Bari, Italy*
[76c] *Politecnico di Bari, Bari, Italy*
[77a] *INFN Sezione di Bologna, Bologna, Italy*
[77b] *Università di Bologna, Bologna, Italy*
[78a] *INFN Sezione di Catania, Catania, Italy*
[78b] *Università di Catania, Catania, Italy*
[79a] *INFN Sezione di Firenze, Firenze, Italy*
[79b] *Università di Firenze, Firenze, Italy*
[80] *INFN Laboratori Nazionali di Frascati, Frascati, Italy*
[81a] *INFN Sezione di Genova, Genova, Italy*
[81b] *Università di Genova, Genova, Italy*
[82a] *INFN Sezione di Milano-Bicocca, Milano, Italy*
[82b] *Università di Milano-Bicocca, Milano, Italy*
[83a] *INFN Sezione di Napoli, Napoli, Italy*
[83b] *Università di Napoli 'Federico II', Napoli, Italy*
[83c] *Università della Basilicata, Potenza, Italy*
[83d] *Scuola Superiore Meridionale (SSM), Napoli, Italy*
[84a] *INFN Sezione di Padova, Padova, Italy*
[84b] *Università di Padova, Padova, Italy*
[84c] *Universita degli Studi di Cagliari, Cagliari, Italy*
[85a] *INFN Sezione di Pavia, Pavia, Italy*
[85b] *Università di Pavia, Pavia, Italy*
[86a] *INFN Sezione di Perugia, Perugia, Italy*
[86b] *Università di Perugia, Perugia, Italy*
[87a] *INFN Sezione di Pisa, Pisa, Italy*
[87b] *Università di Pisa, Pisa, Italy*
[87c] *Scuola Normale Superiore di Pisa, Pisa, Italy*
[87d] *Università di Siena, Siena, Italy*
[88a] *INFN Sezione di Roma, Roma, Italy*
[88b] *Sapienza Università di Roma, Roma, Italy*
[89a] *INFN Sezione di Torino, Torino, Italy*
[89b] *Università di Torino, Torino, Italy*
[89c] *Università del Piemonte Orientale, Novara, Italy*
[90a] *INFN Sezione di Trieste, Trieste, Italy*
[90b] *Università di Trieste, Trieste, Italy*
[91] *Kyungpook National University, Daegu, Korea*
[92] *Department of Mathematics and Physics – GWNU, Gangneung, Korea*
[93] *Chonnam National University, Institute for Universe and Elementary Particles, Kwangju, Korea*
[94] *Hanyang University, Seoul, Korea*
[95] *Korea University, Seoul, Korea*
[96] *Kyung Hee University, Department of Physics, Seoul, Korea*
[97] *Sejong University, Seoul, Korea*
[98] *Seoul National University, Seoul, Korea*
[99] *University of Seoul, Seoul, Korea*

JHEP05(2026)191

[100] *Yonsei University, Department of Physics, Seoul, Korea*
[101] *Sungkyunkwan University, Suwon, Korea*
[102] *College of Engineering and Technology, American University of the Middle East (AUM), Dasman, Kuwait*
[103] *Kuwait University – College of Science – Department of Physics, Safat, Kuwait*
[104] *Riga Technical University, Riga, Latvia*
[105] *University of Latvia (LU), Riga, Latvia*
[106] *Vilnius University, Vilnius, Lithuania*
[107] *National Centre for Particle Physics, Universiti Malaya, Kuala Lumpur, Malaysia*
[108] *Universidad de Sonora (UNISON), Hermosillo, Mexico*
[109] *Centro de Investigacion y de Estudios Avanzados del IPN, Mexico City, Mexico*
[110] *Universidad Iberoamericana, Mexico City, Mexico*
[111] *Benemerita Universidad Autonoma de Puebla, Puebla, Mexico*
[112] *University of Montenegro, Podgorica, Montenegro*
[113] *University of Canterbury, Christchurch, New Zealand*
[114] *National Centre for Physics, Quaid-I-Azam University, Islamabad, Pakistan*
[115] *AGH University of Krakow, Krakow, Poland*
[116] *National Centre for Nuclear Research, Swierk, Poland*
[117] *Institute of Experimental Physics, Faculty of Physics, University of Warsaw, Warsaw, Poland*
[118] *Warsaw University of Technology, Warsaw, Poland*
[119] *Laboratório de Instrumentação e Física Experimental de Partículas, Lisboa, Portugal*
[120] *Faculty of Physics, University of Belgrade, Belgrade, Serbia*
[121] *VINCA Institute of Nuclear Sciences, University of Belgrade, Belgrade, Serbia*
[122] *Centro de Investigaciones Energéticas Medioambientales y Tecnológicas (CIEMAT), Madrid, Spain*
[123] *Universidad Autónoma de Madrid, Madrid, Spain*
[124] *Universidad de Oviedo, Instituto Universitario de Ciencias y Tecnologías Espaciales de Asturias (ICTEA), Oviedo, Spain*
[125] *Instituto de Física de Cantabria (IFCA), CSIC-Universidad de Cantabria, Santander, Spain*
[126] *University of Colombo, Colombo, Sri Lanka*
[127] *University of Ruhuna, Department of Physics, Matara, Sri Lanka*
[128] *CERN, European Organization for Nuclear Research, Geneva, Switzerland*
[129] *PSI Center for Neutron and Muon Sciences, Villigen, Switzerland*
[130] *ETH Zurich – Institute for Particle Physics and Astrophysics (IPA), Zurich, Switzerland*
[131] *Universität Zürich, Zurich, Switzerland*
[132] *National Central University, Chung-Li, Taiwan*
[133] *National Taiwan University (NTU), Taipei, Taiwan*
[134] *High Energy Physics Research Unit, Department of Physics, Faculty of Science, Chulalongkorn University, Bangkok, Thailand*
[135] *Tunis El Manar University, Tunis, Tunisia*
[136] *Çukurova University, Physics Department, Science and Art Faculty, Adana, Turkey*
[137] *Hacettepe University, Ankara, Turkey*
[138] *Middle East Technical University, Physics Department, Ankara, Turkey*
[139] *Bogazici University, Istanbul, Turkey*
[140] *Istanbul Technical University, Istanbul, Turkey*
[141] *Istanbul University, Istanbul, Turkey*
[142] *Yildiz Technical University, Istanbul, Turkey*
[143] *Institute for Scintillation Materials of National Academy of Science of Ukraine, Kharkiv, Ukraine*
[144] *National Science Centre, Kharkiv Institute of Physics and Technology, Kharkiv, Ukraine*
[145] *University of Bristol, Bristol, U.K.*
[146] *Rutherford Appleton Laboratory, Didcot, U.K.*
[147] *Imperial College, London, U.K.*
[148] *Brunel University, Uxbridge, U.K.*
[149] *Baylor University, Waco, Texas, U.S.A.*
[150] *Bethel University, St. Paul, Minnesota, U.S.A.*

JHEP05(2026)191

[151] *Catholic University of America, Washington, DC, U.S.A.*
[152] *The University of Alabama, Tuscaloosa, Alabama, U.S.A.*
[153] *Boston University, Boston, Massachusetts, U.S.A.*
[154] *Brown University, Providence, Rhode Island, U.S.A.*
[155] *University of California, Davis, Davis, California, U.S.A.*
[156] *University of California, Los Angeles, California, U.S.A.*
[157] *University of California, Riverside, Riverside, California, U.S.A.*
[158] *University of California, San Diego, La Jolla, California, U.S.A.*
[159] *University of California, Santa Barbara – Department of Physics, Santa Barbara, California, U.S.A.*
[160] *California Institute of Technology, Pasadena, California, U.S.A.*
[161] *Carnegie Mellon University, Pittsburgh, Pennsylvania, U.S.A.*
[162] *University of Colorado Boulder, Boulder, Colorado, U.S.A.*
[163] *Cornell University, Ithaca, New York, U.S.A.*
[164] *Fermi National Accelerator Laboratory, Batavia, Illinois, U.S.A.*
[165] *University of Florida, Gainesville, Florida, U.S.A.*
[166] *Florida State University, Tallahassee, Florida, U.S.A.*
[167] *Florida Institute of Technology, Melbourne, Florida, U.S.A.*
[168] *University of Illinois Chicago, Chicago, Illinois, U.S.A.*
[169] *The University of Iowa, Iowa City, Iowa, U.S.A.*
[170] *Johns Hopkins University, Baltimore, Maryland, U.S.A.*
[171] *The University of Kansas, Lawrence, Kansas, U.S.A.*
[172] *Kansas State University, Manhattan, Kansas, U.S.A.*
[173] *University of Maryland, College Park, Maryland, U.S.A.*
[174] *Massachusetts Institute of Technology, Cambridge, Massachusetts, U.S.A.*
[175] *University of Minnesota, Minneapolis, Minnesota, U.S.A.*
[176] *University of Nebraska-Lincoln, Lincoln, Nebraska, U.S.A.*
[177] *State University of New York at Buffalo, Buffalo, New York, U.S.A.*
[178] *Northeastern University, Boston, Massachusetts, U.S.A.*
[179] *Northwestern University, Evanston, Illinois, U.S.A.*
[180] *University of Notre Dame, Notre Dame, Indiana, U.S.A.*
[181] *The Ohio State University, Columbus, Ohio, U.S.A.*
[182] *Princeton University, Princeton, New Jersey, U.S.A.*
[183] *University of Puerto Rico, Mayaguez, Puerto Rico, U.S.A.*
[184] *Purdue University, West Lafayette, Indiana, U.S.A.*
[185] *Purdue University Northwest, Hammond, Indiana, U.S.A.*
[186] *Rice University, Houston, Texas, U.S.A.*
[187] *University of Rochester, Rochester, New York, U.S.A.*
[188] *Rutgers, The State University of New Jersey, Piscataway, New Jersey, U.S.A.*
[189] *University of Tennessee, Knoxville, Tennessee, U.S.A.*
[190] *Texas A&M University, College Station, Texas, U.S.A.*
[191] *Texas Tech University, Lubbock, Texas, U.S.A.*
[192] *Vanderbilt University, Nashville, Tennessee, U.S.A.*
[193] *University of Virginia, Charlottesville, Virginia, U.S.A.*
[194] *Wayne State University, Detroit, Michigan, U.S.A.*
[195] *University of Wisconsin – Madison, Madison, Wisconsin, U.S.A.*
[196] *An institute or international laboratory covered by a cooperation agreement with CERN*
[197] *An institute formerly covered by a cooperation agreement with CERN*

[a] *Also at Yerevan State University, Yerevan, Armenia*
[b] *Also at TU Wien, Vienna, Austria*
[c] *Also at Ghent University, Ghent, Belgium*
[d] *Also at FACAMP – Faculdades de Campinas, Sao Paulo, Brazil*
[e] *Also at Universidade do Estado do Rio de Janeiro, Rio de Janeiro, Brazil*

JHEP05(2026)191

[f] Also at Universidade Estadual de Campinas, Campinas, Brazil
[g] Also at Federal University of Rio Grande do Sul, Porto Alegre, Brazil
[h] Also at The University of the State of Amazonas, Manaus, Brazil
[i] Also at University of Chinese Academy of Sciences, Beijing, China
[j] Also at China Center of Advanced Science and Technology, Beijing, China
[k] Also at University of Chinese Academy of Sciences, Beijing, China
[l] Also at School of Physics, Zhengzhou University, Zhengzhou, China
[m] Now at Henan Normal University, Xinxiang, China
[n] Also at University of Shanghai for Science and Technology, Shanghai, China
[o] Now at The University of Iowa, Iowa City, Iowa, U.S.A.
[p] Also at Center for High Energy Physics, Peking University, Beijing, China
[q] Now at British University in Egypt, Cairo, Egypt
[r] Now at Cairo University, Cairo, Egypt
[s] Also at Purdue University, West Lafayette, Indiana, U.S.A.
[t] Also at Université de Haute Alsace, Mulhouse, France
[u] Also at Tbilisi State University, Tbilisi, Georgia
[v] Also at Another institute or international laboratory covered by a cooperation agreement with CERN
[w] Also at University of Hamburg, Hamburg, Germany
[x] Also at RWTH Aachen University, III. Physikalisches Institut A, Aachen, Germany
[y] Also at Bergische University Wuppertal (BUW), Wuppertal, Germany
[z] Also at Brandenburg University of Technology, Cottbus, Germany
[aa] Also at Forschungszentrum Jülich, Juelich, Germany
[ab] Now at RWTH Aachen University, III. Physikalisches Institut A, Aachen, Germany
[ac] Also at CERN, European Organization for Nuclear Research, Geneva, Switzerland
[ad] Also at HUN-REN ATOMKI – Institute of Nuclear Research, Debrecen, Hungary
[ae] Now at Universitatea Babes-Bolyai – Facultatea de Fizica, Cluj-Napoca, Romania
[af] Also at MTA-ELTE Lendület CMS Particle and Nuclear Physics Group, Eötvös Loránd University, Budapest, Hungary
[ag] Also at HUN-REN Wigner Research Centre for Physics, Budapest, Hungary
[ah] Also at Physics Department, Faculty of Science, Assiut University, Assiut, Egypt
[ai] Also at The University of Kansas, Lawrence, Kansas, U.S.A.
[aj] Also at Punjab Agricultural University, Ludhiana, India
[ak] Also at University of Hyderabad, Hyderabad, India
[al] Also at Indian Institute of Science (IISc), Bangalore, India
[am] Also at University of Visva-Bharati, Santiniketan, India
[an] Also at IIT Bhubaneswar, Bhubaneswar, India
[ao] Also at Institute of Physics, Bhubaneswar, India
[ap] Also at Deutsches Elektronen-Synchrotron, Hamburg, Germany
[aq] Also at Isfahan University of Technology, Isfahan, Iran
[ar] Also at Sharif University of Technology, Tehran, Iran
[as] Also at Department of Physics, University of Science and Technology of Mazandaran, Behshahr, Iran
[at] Also at Department of Physics, Faculty of Science, Arak University, ARAK, Iran
[au] Also at Helwan University, Cairo, Egypt
[av] Also at Italian National Agency for New Technologies, Energy and Sustainable Economic Development, Bologna, Italy
[aw] Also at Centro Siciliano di Fisica Nucleare e di Struttura Della Materia, Catania, Italy
[ax] Also at Università degli Studi Guglielmo Marconi, Roma, Italy
[ay] Also at Scuola Superiore Meridionale, Università di Napoli 'Federico II', Napoli, Italy
[az] Also at Fermi National Accelerator Laboratory, Batavia, Illinois, U.S.A.
[ba] Also at Lulea University of Technology, Lulea, Sweden
[bb] Also at Consiglio Nazionale delle Ricerche – Istituto Officina dei Materiali, Perugia, Italy
[bc] Also at UPES – University of Petroleum and Energy Studies, Dehradun, India
[bd] Also at Institut de Physique des 2 Infinis de Lyon (IP2I), Villeurbanne, France

JHEP05(2026)191

[be] Also at Department of Applied Physics, Faculty of Science and Technology, Universiti Kebangsaan Malaysia, Bangi, Malaysia
[bf] Also at Trincomalee Campus, Eastern University, Sri Lanka, Nilaveli, Sri Lanka
[bg] Also at Saegis Campus, Nugegoda, Sri Lanka
[bh] Also at National and Kapodistrian University of Athens, Athens, Greece
[bi] Also at Ecole Polytechnique Fédérale Lausanne, Lausanne, Switzerland
[bj] Also at Universität Zürich, Zurich, Switzerland
[bk] Also at Stefan Meyer Institute for Subatomic Physics, Vienna, Austria
[bl] Also at Near East University, Research Center of Experimental Health Science, Mersin, Turkey
[bm] Also at Konya Technical University, Konya, Turkey
[bn] Also at Izmir Bakircay University, Izmir, Turkey
[bo] Also at Adiyaman University, Adiyaman, Turkey
[bp] Also at Bozok Universitetesi Rektörlügü, Yozgat, Turkey
[bq] Also at Istanbul Sabahattin Zaim University, Istanbul, Turkey
[br] Also at Marmara University, Istanbul, Turkey
[bs] Also at Milli Savunma University, Istanbul, Turkey
[bt] Also at Informatics and Information Security Research Center, Gebze/Kocaeli, Turkey
[bu] Also at Kafkas University, Kars, Turkey
[bv] Now at Istanbul Okan University, Istanbul, Turkey
[bw] Also at Istanbul University – Cerrahpasa, Faculty of Engineering, Istanbul, Turkey
[bx] Also at Istinye University, Istanbul, Turkey
[by] Also at Yildiz Technical University, Istanbul, Turkey
[bz] Also at School of Physics and Astronomy, University of Southampton, Southampton, U.K.
[ca] Also at Monash University, Faculty of Science, Clayton, Australia
[cb] Also at Università di Torino, Torino, Italy
[cc] Also at Karamanoğlu Mehmetbey University, Karaman, Turkey
[cd] Also at California Lutheran University;, Thousand Oaks, California, U.S.A.
[ce] Also at California Institute of Technology, Pasadena, California, U.S.A.
[cf] Also at United States Naval Academy, Annapolis, Maryland, U.S.A.
[cg] Also at Bingol University, Bingol, Turkey
[ch] Also at Georgian Technical University, Tbilisi, Georgia
[ci] Also at Sinop University, Sinop, Turkey
[cj] Also at Erciyes University, Kayseri, Turkey
[ck] Also at Horia Hulubei National Institute of Physics and Nuclear Engineering (IFIN-HH), Bucharest, Romania
[cl] Now at Another institute formerly covered by a cooperation agreement with CERN
[cm] Also at Another institute formerly covered by a cooperation agreement with CERN
[cn] Also at Hamad Bin Khalifa University (HBKU), Doha, Qatar
[co] Also at Yerevan Physics Institute, Yerevan, Armenia
[cp] Also at Imperial College, London, U.K.
[cq] Now at Yerevan Physics Institute, Yerevan, Armenia
[†] Deceased

JHEP05(2026)191